

EUROPEAN LABORATORY FOR PARTICLE PHYSICS (CERN)

CERN-EP/99-093

8 July, 1999

Search for R-Parity Violating Decays of Supersymmetric Particles in e^+e^- Collisions at Centre-of-Mass Energies near 183 GeV

The ALEPH Collaboration

Abstract

Searches for pair-production of supersymmetric particles under the assumption that R-parity is violated via a single dominant $LL\bar{E}$, $LQ\bar{D}$ or $\bar{U}\bar{D}\bar{D}$ coupling are performed using the data collected by the ALEPH collaboration at centre-of-mass energies of 181–184 GeV. The observed candidate events in the data are in agreement with the Standard Model expectations. Upper limits on the production cross-sections and lower limits on the masses of charginos, sleptons, squarks and sneutrinos are derived.

(Submitted to European Physical Journal C)

The ALEPH Collaboration

R. Barate, D. Decamp, P. Ghez, C. Goy, S. Jezequel, J.-P. Lees, F. Martin, E. Merle, M.-N. Minard, B. Pietrzyk, H. Przysiezniak

Laboratoire de Physique des Particules (LAPP), IN²P³-CNRS, F-74019 Annecy-le-Vieux Cedex, France

R. Alemany, M.P. Casado, M. Chmeissani, J.M. Crespo, E. Fernandez, M. Fernandez-Bosman, Ll. Garrido,¹⁵ E. Graugès, A. Juste, M. Martinez, G. Merino, R. Miquel, Ll.M. Mir, P. Morawitz, A. Pacheco, I.C. Park, I. Riu

Institut de Física d'Altes Energies, Universitat Autònoma de Barcelona, 08193 Bellaterra (Barcelona), E-Spain⁷

A. Colaleo, D. Creanza, M. de Palma, G. Iaselli, G. Maggi, M. Maggi, S. Nuzzo, A. Ranieri, G. Raso, F. Ruggieri, G. Selvaggi, L. Silvestris, P. Tempesta, A. Tricomi,³ G. Zito

Dipartimento di Fisica, INFN Sezione di Bari, I-70126 Bari, Italy

X. Huang, J. Lin, Q. Ouyang, T. Wang, Y. Xie, R. Xu, S. Xue, J. Zhang, L. Zhang, W. Zhao

Institute of High-Energy Physics, Academia Sinica, Beijing, The People's Republic of China⁸

D. Abbaneo, U. Becker,¹⁹ G. Boix,⁶ M. Cattaneo, F. Cerutti, V. Ciulli, G. Dissertori, H. Drevermann, R.W. Forty, M. Frank, F. Gianotti, T.C. Greening, A.W. Halley, J.B. Hansen, J. Harvey, P. Janot, B. Jost, I. Lehraus, O. Leroy, C. Loomis, P. Maley, P. Mato, A. Minten, A. Moutoussi, F. Ranjard, L. Rolandi, D. Schlatter, M. Schmitt,²⁰ O. Schneider,² P. Spagnolo, W. Tejessy, F. Teubert, I.R. Tomalin, E. Tournefier, A.E. Wright

European Laboratory for Particle Physics (CERN), CH-1211 Geneva 23, Switzerland

Z. Ajaltouni, F. Badaud, G. Chazelle, O. Deschamps, S. Dessagne, A. Falvard, C. Ferdi, P. Gay, C. Guicheney, P. Henrard, J. Jousset, B. Michel, S. Monteil, J.-C. Montret, D. Pallin, P. Perret, F. Podlyski

Laboratoire de Physique Corpusculaire, Université Blaise Pascal, IN²P³-CNRS, Clermont-Ferrand, F-63177 Aubière, France

J.D. Hansen, J.R. Hansen, P.H. Hansen, B.S. Nilsson, B. Rensch, A. Wäänänen

Niels Bohr Institute, 2100 Copenhagen, DK-Denmark⁹

G. Daskalakis, A. Kyriakis, C. Markou, E. Simopoulou, A. Vayaki

Nuclear Research Center Demokritos (NRCD), GR-15310 Attiki, Greece

A. Blondel, J.-C. Brient, F. Machefert, A. Rougé, M. Swynghedauw, R. Tanaka, A. Valassi,²³ H. Videau

Laboratoire de Physique Nucléaire et des Hautes Energies, Ecole Polytechnique, IN²P³-CNRS, F-91128 Palaiseau Cedex, France

E. Focardi, G. Parrini, K. Zachariadou

Dipartimento di Fisica, Università di Firenze, INFN Sezione di Firenze, I-50125 Firenze, Italy

R. Cavanaugh, M. Corden, C. Georgopoulos

Supercomputer Computations Research Institute, Florida State University, Tallahassee, FL 32306-4052, USA^{13,14}

A. Antonelli, G. Bencivenni, G. Bologna,⁴ F. Bossi, P. Campana, G. Capon, V. Chiarella, P. Laurelli, G. Mannocchi,^{1,5} F. Murtas, G.P. Murtas, L. Passalacqua, M. Pepe-Altarelli¹

Laboratori Nazionali dell'INFN (LNF-INFN), I-00044 Frascati, Italy

M. Chalmers, L. Curtis, J.G. Lynch, P. Negus, V. O'Shea, B. Raeven, C. Raine, D. Smith, P. Teixeira-Dias, A.S. Thompson, J.J. Ward

Department of Physics and Astronomy, University of Glasgow, Glasgow G12 8QQ, United Kingdom¹⁰

O. Buchmüller, S. Dhamotharan, C. Geweniger, P. Hanke, G. Hansper, V. Hepp, E.E. Kluge, A. Putzer, J. Sommer, K. Tittel, S. Werner,¹⁹ M. Wunsch

Institut für Hochenergiephysik, Universität Heidelberg, D-69120 Heidelberg, Germany¹⁶

R. Beuselinck, D.M. Binnie, W. Cameron, P.J. Dornan,¹ M. Girone, S. Goodsir, N. Marinelli, E.B. Martin, J. Nash, J. Nowell, A. Sciabà, J.K. Sedgbeer, E. Thomson, M.D. Williams

Department of Physics, Imperial College, London SW7 2BZ, United Kingdom¹⁰

V.M. Ghete, P. Girtler, E. Kneringer, D. Kuhn, G. Rudolph

Institut für Experimentalphysik, Universität Innsbruck, A-6020 Innsbruck, Austria¹⁸

C.K. Bowdery, P.G. Buck, G. Ellis, A.J. Finch, F. Foster, G. Hughes, R.W.L. Jones, N.A. Robertson, M. Smizanska, M.I. Williams

Department of Physics, University of Lancaster, Lancaster LA1 4YB, United Kingdom¹⁰

I. Giehl, F. Hölldorfer, K. Jakobs, K. Kleinknecht, M. Kröcker, A.-S. Müller, H.-A. Nürnbergger, G. Quast, B. Renk, E. Rohne, H.-G. Sander, S. Schmeling, H. Wachsmuth C. Zeitnitz, T. Ziegler

Institut für Physik, Universität Mainz, D-55099 Mainz, Germany¹⁶

J.J. Aubert, C. Benchouk, A. Bonissent, J. Carr,¹ P. Coyle, A. Ealet, D. Fouchez, F. Motsch, P. Payre, D. Rousseau, M. Talby, M. Thulasidas, A. Tilquin

Centre de Physique des Particules, Faculté des Sciences de Luminy, IN²P³-CNRS, F-13288 Marseille, France

M. Aleppo, M. Antonelli, F. Ragusa

Dipartimento di Fisica, Università di Milano e INFN Sezione di Milano, I-20133 Milano, Italy.

V. Büscher, H. Dietl, G. Ganis, K. Hüttmann, G. Lütjens, C. Mannert, W. Männer, H.-G. Moser, S. Schael, R. Settles, H. Seywerd, H. Stenzel, W. Wiedenmann, G. Wolf

Max-Planck-Institut für Physik, Werner-Heisenberg-Institut, D-80805 München, Germany¹⁶

P. Azzurri, J. Boucrot, O. Callot, S. Chen, M. Davier, L. Duflot, J.-F. Grivaz, Ph. Heusse, A. Jacholkowska,¹ M. Kado, J. Lefrançois, L. Serin, J.-J. Veillet, I. Videau,¹ J.-B. de Vivie de Régie, D. Zerwas

Laboratoire de l'Accélérateur Linéaire, Université de Paris-Sud, IN²P³-CNRS, F-91898 Orsay Cedex, France

G. Bagliesi, S. Bettarini, T. Boccali, C. Bozzi,¹² G. Calderini, R. Dell'Orso, I. Ferrante, A. Giassi, A. Gregorio, F. Ligabue, A. Lusiani, P.S. Marrocchesi, A. Messineo, F. Palla, G. Rizzo, G. Sanguinetti, G. Sguazzoni, R. Tenchini, C. Vannini, A. Venturi, P.G. Verdini

Dipartimento di Fisica dell'Università, INFN Sezione di Pisa, e Scuola Normale Superiore, I-56010 Pisa, Italy

G.A. Blair, J. Coles, G. Cowan, M.G. Green, D.E. Hutchcroft, L.T. Jones, T. Medcalf, J.A. Strong, J.H. von Wimmersperg-Toeller

Department of Physics, Royal Holloway & Bedford New College, University of London, Surrey TW20 OEX, United Kingdom¹⁰

D.R. Botterill, R.W. Clift, T.R. Edgecock, P.R. Norton, J.C. Thompson

Particle Physics Dept., Rutherford Appleton Laboratory, Chilton, Didcot, Oxon OX11 0QX, United Kingdom¹⁰

B. Bloch-Devaux, P. Colas, B. Fabbro, G. Faïf, E. Lançon, M.-C. Lemaire, E. Locci, P. Perez, J. Rander, J.-F. Renardy, A. Rosowsky, A. Trabelsi,²¹ B. Tuchming, B. Vallage

CEA, DAPNIA/Service de Physique des Particules, CE-Saclay, F-91191 Gif-sur-Yvette Cedex, France¹⁷

S.N. Black, J.H. Dann, H.Y. Kim, N. Konstantinidis, A.M. Litke, M.A. McNeil, G. Taylor

Institute for Particle Physics, University of California at Santa Cruz, Santa Cruz, CA 95064, USA²²

C.N. Booth, S. Cartwright, F. Combley, P.N. Hodgson, M.S. Kelly, M. Lehto, L.F. Thompson
*Department of Physics, University of Sheffield, Sheffield S3 7RH, United Kingdom*¹⁰

K. Affholderbach, A. Böhrer, S. Brandt, C. Grupen, J. Hess, A. Misiejuk, G. Prange, U. Sieler
*Fachbereich Physik, Universität Siegen, D-57068 Siegen, Germany*¹⁶

G. Giannini, B. Gobbo
Dipartimento di Fisica, Università di Trieste e INFN Sezione di Trieste, I-34127 Trieste, Italy

J. Putz, J. Rothberg, S. Wasserbaech, R.W. Williams
Experimental Elementary Particle Physics, University of Washington, WA 98195 Seattle, U.S.A.

S.R. Armstrong, P. Elmer, D.P.S. Ferguson, Y. Gao, S. González, O.J. Hayes, H. Hu, S. Jin, P.A. McNamara
III, J. Nielsen, W. Orejudos, Y.B. Pan, Y. Saadi, I.J. Scott, J. Walsh, Sau Lan Wu, X. Wu, G. Zobernig
*Department of Physics, University of Wisconsin, Madison, WI 53706, USA*¹¹

¹Also at CERN, 1211 Geneva 23, Switzerland.

²Now at Université de Lausanne, 1015 Lausanne, Switzerland.

³Also at Centro Siciliano di Fisica Nucleare e Struttura della Materia, INFN Sezione di Catania, 95129 Catania, Italy.

⁴Also Istituto di Fisica Generale, Università di Torino, 10125 Torino, Italy.

⁵Also Istituto di Cosmo-Geofisica del C.N.R., Torino, Italy.

⁶Supported by the Commission of the European Communities, contract ERBFMBICT982894.

⁷Supported by CICYT, Spain.

⁸Supported by the National Science Foundation of China.

⁹Supported by the Danish Natural Science Research Council.

¹⁰Supported by the UK Particle Physics and Astronomy Research Council.

¹¹Supported by the US Department of Energy, grant DE-FG0295-ER40896.

¹²Now at INFN Sezione di Ferrara, 44100 Ferrara, Italy.

¹³Supported by the US Department of Energy, contract DE-FG05-92ER40742.

¹⁴Supported by the US Department of Energy, contract DE-FC05-85ER250000.

¹⁵Permanent address: Universitat de Barcelona, 08208 Barcelona, Spain.

¹⁶Supported by the Bundesministerium für Bildung, Wissenschaft, Forschung und Technologie, Germany.

¹⁷Supported by the Direction des Sciences de la Matière, C.E.A.

¹⁸Supported by Fonds zur Förderung der wissenschaftlichen Forschung, Austria.

¹⁹Now at SAP AG, 69185 Walldorf, Germany

²⁰Now at Harvard University, Cambridge, MA 02138, U.S.A.

²¹Now at Département de Physique, Faculté des Sciences de Tunis, 1060 Le Belvédère, Tunisia.

²²Supported by the US Department of Energy, grant DE-FG03-92ER40689.

²³Now at LAL, 91898 Orsay, France.

1 Introduction

Minimal supersymmetric extensions of the Standard Model (MSSM) [1] usually assume that R-parity is conserved [2]. R-parity is defined as $R_p = -1^{3B+L+2S}$ where B denotes the baryon number, L the lepton number and S the spin of a field. Conservation of R-parity forbids the presence of the following L or B violating terms in the superpotential [3]:

$$W_{\mathcal{R}_p} = \lambda_{ijk} L_i L_j \bar{E}_k + \lambda'_{ijk} L_i Q_j \bar{D}_k + \lambda''_{ijk} \bar{U}_i \bar{D}_j \bar{D}_k. \quad (1)$$

Here \bar{D}, \bar{U} (\bar{E}) are the down-like and up-like quark (lepton) singlet superfields, and L (Q) are the lepton (quark) doublet superfields respectively; λ, λ' , and λ'' are Yukawa couplings, and $i, j, k = 1, 2, 3$ are generation indices. The λ term is anti-symmetric in i and j and the λ'' term is anti-symmetric in j and k giving rise to a total of $9\lambda + 27\lambda' + 9\lambda'' = 45$ new parameters.

Phenomenologically viable models, in which only subsets of the terms in Equation (1) are non-zero are also possible [4] and lead to decay topologies not covered by the R-parity conserving analyses. This paper considers the possible pair-production of Supersymmetric particles at LEP 2 and their subsequent R-parity violating decays. The following assumptions are made throughout:

- All three terms in Equation (1) are addressed, but models in which more than one term is non-zero are not considered. When the results are translated into limits, it is also assumed that the couplings are non-zero for only one choice of i, j and k . Unless otherwise stated the derived limits correspond to the choice of indices for the coupling giving the worst limit.
- The lifetimes of the decaying sparticles are negligible, i.e. their average decay length is less than 1 cm.
- Results are interpreted within the framework of the MSSM. The unification relation $M_1 = \frac{5}{3} M_2 \tan^2 \theta_W$ is assumed.
- For the case of the charginos and neutralinos, only large values of the universal scalar mass (m_0) are considered and it is therefore assumed that the lightest neutralino is the LSP. Low m_0 scenarios for the cases of non-zero $LL\bar{E}$ and $LQ\bar{D}$ couplings were considered at lower centre of mass energies, in Refs. [5] and [6] respectively.

The search results reported here use 56.9 pb^{-1} of data collected by ALEPH in 1997 at centre-of-mass energies from 181 to 184 GeV. New searches for $\bar{U}\bar{D}\bar{D}$ topologies are presented and the previously published ALEPH $LL\bar{E}$ and $LQ\bar{D}$ analyses [5, 6] are updated to include the new data.

The organisation of the paper is as follows: in Section 2 the phenomenology of R-parity violating decays is discussed and then in Section 3 existing limits from lower energy measurements are summarised. After a brief description of the ALEPH detector

in Section 4, the Monte Carlo samples used are described in Section 5. In Sections 6, 7 and 8 the selections, results and their interpretation within the MSSM are discussed for each of the R-parity violating operators. Finally a summary is given in Section 9.

2 Phenomenology

The various possible decay modes of all supersymmetric particles, *sparticles*, are grouped into two categories. Decays proceeding via the lightest neutralino are referred to as the *indirect* decay modes; decays directly to Standard Model particles are referred to as *direct* decay modes. The sparticle decay modes studied are summarised in Table 1, and decay diagrams of the *direct* decay modes considered are shown in Figure 1. As indicated in Table 1, the flavours of the final state fermions depend upon the type and the flavour structure of the Yukawa coupling.

Under the assumption of large m_0 , the *indirect* decays of the lightest chargino and the next-to-lightest neutralino, into $W^*\chi$ and $Z^*\chi$ respectively, dominate over the *direct* decay modes; the latter are suppressed by the large sfermion masses and are not considered here. The assumption of large m_0 also implies that for the neutralino decay, the intermediate sparticle is virtual and therefore the decay kinematics is three body.

Sfermions can decay *indirectly* via the lightest neutralino: $\tilde{l} \rightarrow l\chi$, $\tilde{\nu} \rightarrow \nu\chi$ and $\tilde{q} \rightarrow q\chi$. If the chargino is lighter than the sfermions, the decays $\tilde{l} \rightarrow \nu\chi^+$, $\tilde{\nu} \rightarrow l^-\chi^+$ and $\tilde{q} \rightarrow q'\chi^+$ are viable decay modes, but are not considered in the following. Sfermions may also decay *directly* to two fermions.

More detailed discussion of the various decay topologies are given in the relevant Sections.

3 Existing limits

An explicit search at LEP 1 for sparticles decaying via the $LL\bar{E}$ coupling [7] yielded $M_{\tilde{l}} > 45 \text{ GeV}/c^2$ and $M_{\tilde{\nu}} > 46 \text{ GeV}/c^2$ for sleptons and sneutrinos. The limit for squarks is $M_{\tilde{q}} > 45 \text{ GeV}/c^2$ when $\phi_{\text{mix}} = 0^\circ$ for both left and right handed states. For the lightest stop the limit is $M_{\tilde{t}_1} > 41 \text{ GeV}/c^2$ assuming the most conservative choice of mixing angle ($\phi_{\text{mix}} = 56^\circ$). Although no explicit searches for sparticles decaying via a dominant $LQ\bar{D}$ or $\bar{U}\bar{D}\bar{D}$ coupling have been performed at LEP 1, constraints [6] from the precision measurement of Γ_Z are applicable for any R-parity violating coupling and yield: $M_{\chi^\pm} > 45 \text{ GeV}/c^2$, $M_{\tilde{l}} > 38 \text{ GeV}/c^2$, $M_{\tilde{\nu}} > 41 \text{ GeV}/c^2$ and $M_{\tilde{q}_L} > 44 \text{ GeV}/c^2$.

Limits from previous LEP 2 searches, gave $M_{\chi^\pm} > 85, 85$ and $76 \text{ GeV}/c^2$ for the $LL\bar{E}$ [5], $LQ\bar{D}$ [6] and $\bar{U}\bar{D}\bar{D}$ [8] couplings respectively (assuming $m_0 = 500 \text{ GeV}/c^2$). In addition, for the λ coupling a lower limit on the lightest neutralino of $M_\chi > 23 \text{ GeV}/c^2$ has been obtained for any choice of μ , M_2 , m_0 or generation indices i, j, k [5].

Sparticle	Indirect Decay Modes	Direct Decay Modes		
		$LL\bar{E}$ (λ_{ijk})	$LQ\bar{D}$ (λ'_{ijk})	$\bar{U}\bar{D}\bar{D}$ (λ''_{ijk})
χ^+	$f\bar{f}'\chi$	$\nu_i\nu_j l_k^+, l_i^+ l_j^+ l_k^-$ $l_i^+ \nu_j \nu_k, \nu_i l_j^+ \nu_k$	$\nu_i u_j \bar{d}_k, l_i^+ \bar{d}_j d_k$ $l_i^+ \bar{u}_j u_k, \bar{\nu}_i \bar{d}_j u_k$	$\bar{d}_i \bar{d}_j \bar{d}_k, u_i u_j d_k$ $u_i d_j u_k$
χ	-	$l_i^- \bar{\nu}_j l_k^+, l_i^+ \nu_j l_k^-$ $\bar{\nu}_i l_j^- l_k^+, \nu_i l_j^+ l_k^-$	$l_i^- u_j \bar{d}_k, l_i^+ \bar{u}_j d_k$ $\nu_i d_j \bar{d}_k, \bar{\nu}_i \bar{d}_j d_k$	$u_i d_j d_k, \bar{u}_i \bar{d}_j \bar{d}_k$
χ'	$f\bar{f}\chi$	$l_i^- \bar{\nu}_j l_k^+, l_i^+ \nu_j l_k^-$ $\bar{\nu}_i l_j^- l_k^+, \nu_i l_j^+ l_k^-$	$l_i^- u_j \bar{d}_k, l_i^+ \bar{u}_j d_k$ $\nu_i d_j \bar{d}_k, \bar{\nu}_i \bar{d}_j d_k$	$u_i d_j d_k, \bar{u}_i \bar{d}_j \bar{d}_k$
\tilde{d}_{kR}	$d_k\chi$	-	$\bar{\nu}_i d_j, l_i^- u_j$	$\bar{u}_i \bar{d}_j$
\tilde{d}_{jR}	$d_j\chi$	-	-	$\bar{u}_i \bar{d}_k$
\tilde{d}_{jL}	$d_j\chi$	-	$\bar{\nu}_i d_k$	-
\tilde{u}_{jL}	$u_j\chi$	-	$l_i^+ d_k$	-
\tilde{u}_{iR}	$u_i\chi$	-	-	$\bar{d}_j \bar{d}_k$
$\tilde{\ell}_{iL}^-$	$l_i\chi$	$\nu_j l_k^-$	$\bar{u}_j d_k$	-
$\tilde{\ell}_{jL}^-$	$l_j\chi$	$\nu_i l_k^-$	-	-
$\tilde{\ell}_{kR}^-$	$l_k\chi$	$\nu_i l_j^-, \nu_j l_i^-$	-	-
$\tilde{\nu}_i$	$\nu_i\chi$	$l_j^- l_k^+$	$d_j \bar{d}_k$	-
$\tilde{\nu}_j$	$\nu_j\chi$	$l_i^- l_k^+$	-	-

Table 1: Indirect and direct R -parity violating decay modes of supersymmetric particles. Here i, j and k are the generation indices. For example, the left handed selectron can decay via the $LQ\bar{D}$ coupling λ'_{123} , $\tilde{e}_L^- \rightarrow \bar{c}b$. Dashes indicate that no direct decay is possible for that coupling. Only those sfermions that have direct decay modes are shown; all sfermions have indirect decay modes available if kinematically allowed. The direct decay modes of the heavier neutralinos (χ') are identical to those of lightest neutralino (χ).

In addition to the above SUSY mass limits, upper limits on the size of the couplings from low energy measurements also exist [9] and are usually quoted assuming a mass of 100 GeV/ c^2 for the virtual sparticles involved in the R -parity violating processes. Although these limits are often strong for products of couplings (e.g. non-observation of proton decays implies $\lambda'_{11k}\lambda''_{11k} < 10^{-22}$), they are considerably weaker if only one coupling is considered dominant:

- The indirect upper limits on the nine possible λ couplings are in the range $10^{-3} - 10^{-1}$. The most stringent upper limit is $\lambda_{133} < 0.003$, derived from the upper limit on the mass of the electron neutrino.
- The indirect limits on the 27 possible λ' couplings are typically of the order $\lambda' < 10^{-2} - 10^{-1}$. The most stringent upper limit is $\lambda'_{111} < 4.10^{-4}$, from searches for neutrinoless double beta decay.

- Except for the λ''_{112} coupling, which is well constrained by double nucleon decay, ($\lambda''_{112} < 10^{-6}$) the indirect limits provide little constraint on the value of the nine possible λ'' couplings.

For sparticle masses close to the kinematic limit, the assumption of negligible lifetime for the decaying sparticle restricts the sensitivity for this analysis, to coupling values of $10^{-4} - 10^{-5}$ for gauginos and about 10^{-7} for *direct* decay of sfermions[5].

In addition, when combined with the above low energy constraints, the assumption of negligible lifetime also limits the validity of this analysis to $M_\chi \gtrsim 10 \text{ GeV}/c^2$.

4 The ALEPH Detector

The ALEPH detector is described in detail in Ref. [10]. An account of the performance of the detector and a description of the standard analysis algorithms can be found in Ref. [11]. Here, only a brief description of the detector components and the algorithms relevant for this analysis is given.

The trajectories of charged particles are measured with a silicon vertex detector, a cylindrical drift chamber, and a large time projection chamber (TPC). The detectors are immersed in a 1.5 T axial field provided by a superconducting solenoidal coil. The electromagnetic calorimeter (ECAL), placed between the TPC and the coil, is a highly segmented sampling calorimeter which is used to identify electrons and photons and to measure their energy. The luminosity monitors extend the calorimetric coverage down to 34 mrad from the beam axis. The hadron calorimeter (HCAL) consists of the iron return yoke of the magnet instrumented with streamer tubes. It provides a measurement of hadronic energy and, together with the external muon chambers, muon identification. The calorimetry and tracking information are combined in an energy flow algorithm which gives a measure of the total energy, and therefore the missing energy, with an error of $(0.6\sqrt{E} + 0.6) \text{ GeV}$.

Lepton identification is described in Ref.[11]. Electrons are identified using the transverse and longitudinal shower shapes in ECAL. Muons are separated from hadrons by their characteristic pattern in HCAL and the presence of hits in the muon chambers.

5 Monte Carlo Samples and Selection Efficiencies

The signal topologies for the *direct* and *indirect* decays were simulated using the SUSYGEN Monte Carlo (MC) program [12] for a wide range of signal masses. The events were subsequently passed through either a full simulation or a faster simplified simulation of the ALEPH detector. Where the fast simulation is used a subselection of these were also passed through the full simulation to verify the accuracy of the fast simulation and a small correction applied if necessary.

Within **SUSYGEN** the decays of the lightest neutralino via the λ'' coupling to three quarks are simulated using a simplified string fragmentation model, which is expected to underestimate the jet activity in the event [12]. As the $\bar{U}\bar{D}\bar{D}$ selections are optimised to select events with large jet activity, the efficiency estimates for the signal topologies are expected to be slightly underestimated and therefore conservative. This was checked by comparing efficiencies obtained with the simplified string fragmentation model to those obtained with an independent fragmentation model [14].

For the stop, the decays via loop diagrams to a charm quark and the lightest neutralino result in a lifetime larger than the typical hadronisation time scale. The scalar bottom can also develop a substantial lifetime in certain regions of parameter space. It is also possible that the lifetime of squarks decaying *directly* is sufficiently long for hadronisation effects to become important. This has been taken into account by modifying **SUSYGEN** to allow stops and sbottoms to hadronise prior to their decays according to the spectator model [13].

Samples of all major backgrounds have been generated and passed through the full simulation, corresponding to at least 20 times the collected luminosity in the data. Events from $\gamma\gamma \rightarrow$ hadrons, $e^+e^- \rightarrow q\bar{q}$ and four-fermion events from $W\nu$, ZZ and Zee were produced with **PYTHIA** [14], with a vector-boson invariant mass cut of $0.2 \text{ GeV}/c^2$ for ZZ and $W\nu$, and $2 \text{ GeV}/c^2$ for Zee . Pairs of W bosons were generated with **KORALW** [15]. Pair production of leptons was simulated with **UNIBAB** [16] (electrons) and **KORALZ** [17] (muons and taus), and the process $\gamma\gamma \rightarrow$ leptons with **PHOT02** [18].

The selections were optimised to give the minimum *expected* 95% C.L. excluded cross-section (σ_{95}) for signal masses close to the high end of the expected sensitivity [19]. Selection efficiencies are determined as a function of the SUSY particle masses and the generation structure of the R-parity violating couplings λ_{ijk} , λ'_{ijk} and λ''_{ijk} , for *indirect* and, where considered, *direct* decay topologies. When more than one selection is used for a search, the selection yielding the best σ_{95} is chosen.

The systematic uncertainties on the selection efficiencies are of order of 4-5% and are dominated by the statistical uncertainty of the Monte Carlo signal samples, with small additional contributions from lepton identification and energy flow reconstruction. They are taken into account by reducing the selection efficiencies by one standard deviation. Background subtraction is only performed for the ‘‘Four Jets’’ and the ‘‘Acoplanar leptons’’ selections, for which the error on the background estimates is taken into account by reducing the background by one standard deviation.

6 Decays via a dominant $LL\bar{E}$ (λ) Coupling

Under the assumption of a dominant λ coupling, the decay topologies can consist of as little as two acoplanar leptons in the simplest case (*direct* slepton decay), or they may consist of as many as six leptons plus four neutrinos in the more complicated case (*indirect* chargino decay). In addition to the purely leptonic topologies, the MSSM cascade decays of heavier

Selection	Data	Standard Model Expectation	Direct Decays	Indirect Decays
Leptons and Hadrons	7	2.4	χ	χ^\pm, \tilde{q}
6 Leptons + \cancel{E}	0	0.3		\tilde{l}
4 Leptons + \cancel{E}	2	1.0		$\tilde{\nu}$
Acoplanar Leptons	43	48.9	\tilde{l}	
4 Leptons	2	1.3	$\chi, \tilde{\nu}$	

Table 2: *Topologies arising from $LL\bar{E}$ couplings: the selections, the number of candidate events selected in the data, the number of background events expected, and the signal processes giving rise to the above topologies.*

gauginos into lighter gaugino states may produce multi-jet and multi-lepton final states. No *direct* decays are possible for the squarks.

The various selections addressing the above topologies, the corresponding SUSY signals, the expected backgrounds and the candidates selected in the data at $\sqrt{s} = 181 - 184$ GeV are summarised in Table 2. Details of the “6 Leptons + \cancel{E} ”, the “4 Leptons + \cancel{E} ” and the “4 Leptons” analyses are given in Ref. [5]. The “Leptons and Hadrons” and the “Acoplanar Leptons” selection were updated and reoptimised for the higher centre-of-mass energy as described below.

6.1 Chargino and neutralino decaying via $LL\bar{E}$

Depending on the masses of the supersymmetric particles and on the lepton flavour composition in the decay, the *indirect* decays of charginos to neutralinos populate different regions in track multiplicity, visible mass and leptonic energy. For this reason three different subselections were developed [5], covering topologies with large leptonic energies and at least two jets (Subselection I), topologies with small multiplicities and large leptonic energy fractions (Subselection II), and topologies with a moderate leptonic energy fraction (Subselection III). The combination of the three sub-selections is defined as the “Leptons and Hadrons” selection. The complete set of cuts are shown in Table 3, with preselection cuts using the number of charged tracks (N_{ch}), the visible mass (M_{vis}) and the transverse missing momentum (p_{\perp}^{miss}) followed by cuts on the Durham jet algorithm distance (y_i , at the transition between $i-1$ and i jets), the thrust of the event (T), the number of leptons as electrons or muons (N_{lep}) and the energy tagged as leptonic or hadronic (E_{lep} or E_{had}). While the core of this selection is unchanged with respect to Ref. [5], the WW rejection is modified due to the kinematically different properties of this background at $\sqrt{s} = 181 - 184$ GeV by redefining

$$\chi_{WW}^2 = \left(\frac{m_{qq} - m_W}{10 \text{ GeV}/c^2} \right)^2 + \left(\frac{m_{l\nu} - m_W}{10 \text{ GeV}/c^2} \right)^2 + \left(\frac{E_l + \cancel{E} - 94 \text{ GeV}}{10 \text{ GeV}} \right)^2. \quad (2)$$

subselection I	subselection II	subselection III
$N_{\text{ch}} \geq 5$ $M_{\text{vis}} > 25 \text{ GeV}/c^2$	$5 \leq N_{\text{ch}} \leq 15$ $20 \text{ GeV}/c^2 < M_{\text{vis}} < 75\% \sqrt{s}$	$N_{\text{ch}} \geq 11$ $55\% \sqrt{s} < M_{\text{vis}} < 80\% \sqrt{s}$
$p_{\perp}^{\text{miss}} > 3.5\% \sqrt{s}$ $ p_z^{\text{miss}} < 27 \text{ GeV}/c$	$p_{\perp}^{\text{miss}} > 2.5\% \sqrt{s}$	$p_{\perp}^{\text{miss}} > 5\% \sqrt{s}$ $N_{\text{ch}}^{\text{jet}} \geq 1$
$y_5 > 0.006$	$y_3 > 0.009$ $y_4 > 0.0026$	$y_3 > 0.025$ $y_4 > 0.012$ $y_5 > 0.004$ $T < 0.85$
$N_{\text{lep}} \geq 1$ $E_{\text{nonlep}} < 54\% \sqrt{s}$ $E_{\text{had}} < 28\% E_{\text{vis}}$	$N_{\text{lep}} \geq 1$ $E_{\text{nonlep}} < 70\% \sqrt{s}$ $E_{\text{had}} < 22\% E_{\text{lep}}$	$N_{\text{lep}} \geq 1$ $E_{\text{lep}} > 20\% E_{\text{had}}$
$\chi_{WW}^2 > 3.8$		

Table 3: *The list of cuts for the “Leptons and Hadrons” selection, which is used for neutralinos, charginos and squarks decaying indirectly via the $LL\bar{E}$ operator.*

Here m_{qq} is the hadronic mass, i.e. the mass of the event after removing the leading lepton, \cancel{E} the missing energy in the event, $m_{l\nu}$ is the mass of the leading lepton and the missing momentum, and E_l the energy of the leading lepton in the event.

After all cuts a total background of 2.4 events is expected for the inclusive combination of the three subselections, dominantly coming from $WW \rightarrow qq\tau\nu$. In the data 7 events are selected. The probability of observing 7 or more events when 2.4 events are expected is 1.2%. Since the events do not cluster in any particular sub-selection (as would be expected for a signal) and as event properties are consistent with standard model expectations, the excess is interpreted as a statistical fluctuation of the background contamination.

Interpreting these results in the framework of the MSSM, 95% C.L. exclusion limits are derived in the (μ, M_2) plane and shown in Figure 2(a) for large scalar masses $m_0 = 500 \text{ GeV}/c^2$. The corresponding lower limit on the mass of the lightest chargino is essentially at the kinematic limit for pair production.

6.2 Squarks decaying via $LL\bar{E}$

Although squarks cannot decay *directly* with a λ coupling, they may decay *indirectly* to the lightest neutralino. This topology is also selected by the “Leptons and Hadrons” selection. The 95% C.L. exclusion limits on the stop are presented in the $(M_\chi, M_{\tilde{t}})$ plane in Figure 3. Using the bound $M_\chi > 23 \text{ GeV}/c^2$ [5] the following limits upon the left-handed stop can be derived: $M_{\tilde{t}_L} > 61 \text{ GeV}/c^2$ (λ_{133} coupling) and $M_{\tilde{t}_L} > 71 \text{ GeV}/c^2$ (λ_{122} coupling).

Topology	ee	$\mu\mu$	$\tau\tau$	$e\mu$	$e\tau$	$\mu\tau$
WW background	7.9	7.7	4.6	15.8	7.7	8.8
Selected in Data	6	7	4	16	8	8

Table 4: *The events selected in the data by the acoplanar lepton selections, listed according to the topology in which they are selected, and the WW background expectation. Some of the background and candidate events are in common to several selections.*

6.3 Sleptons decaying via $LL\bar{E}$

Sleptons decaying *directly* to a lepton and a neutrino produce acoplanar lepton topologies of same or mixed flavour. For the acoplanar lepton final states ee , $\mu\mu$ and $\tau\tau$ the selections developed for the search for sleptons with R-parity conservation are used [20]. Only those selections designed for large mass differences between the slepton and the lightest neutralino are employed.

The extension of these selections to mixed final states is similar to that in Ref. [5]. For $e\mu$ final states, the requirement for two identified leptons of the same flavour is replaced by the requirement for one electron and one muon. For $e\tau$ ($\mu\tau$), the leading lepton should be an electron (muon) with momentum less than 70 GeV/ c . In case there is a second lepton identified, its momentum should be less than 18 GeV/ c .

Although efficiencies for the acoplanar lepton topologies are high, the expected background in this channel is also large but well modelled, and is therefore subtracted according to the prescription given in Ref. [22].

As described in Ref. [5] right-handed sleptons decay to two final states (if $\lambda_{ijk} \neq 0$ then $\tilde{l}_R^k \rightarrow l^i \bar{\nu}_l^j$ or $\bar{\nu}_l^i l^j$) in the *direct* topology with a 50% branching ratio each for a given choice of the generation indices. Table 4 lists the data and standard model expectation for each possible acoplanar lepton pair. Excluded cross-sections are shown in Figure 4(a) for the appropriate mixtures of acoplanar lepton states. The MSSM production cross-section for right-handed smuon pairs and selectron pairs at $\mu = -200$ GeV/ c^2 and $\tan\beta = 2$ are superimposed. The cross-section limit translates into a lower bound on the smuon (or stau) mass of $M_{\tilde{\mu}_R}, M_{\tilde{\tau}_R} > 61$ GeV/ c^2 and $M_{\tilde{e}_R} > 82$ GeV/ c^2 ($\mu = -200$ GeV/ c^2 , $\tan\beta = 2$) for the *direct* decays and the worst case coupling.

Indirect decays of sleptons are selected using the “Six Leptons + \cancel{E} ” selection. Limits corresponding to this case are shown in Figure 4(b), 4(c) and 4(d). Using the bound of $M_\chi > 23$ GeV/ c^2 obtained in Ref. [5] these limits can be interpreted as the mass limits $M_{\tilde{e}_R} > 76$ GeV/ c^2 ($\mu = -200$ GeV/ c^2 , $\tan\beta = 2$), $M_{\tilde{\mu}_R} > 74$ GeV/ c^2 and $M_{\tilde{\tau}_R} > 70$ GeV/ c^2 for the worst case coupling.

Selection	Data	Standard Model Expectation	Direct Decays	Indirect Decays
MultiJets + Leptons	7	8.7	χ	χ^\pm
Four Jets	144	142.0	$\tilde{l}, \tilde{\nu}$	
2 Jets + 2τ	2	2.6	\tilde{t}_R	
AJ-H	1	0.5	\tilde{b}_L	

Table 5: *Topologies arising from $LQ\bar{D}$ couplings: the selections, the signal processes giving rise to the above topologies, the number of background events expected, and the number of candidate events selected in the data.*

6.4 Sneutrinos decaying via $LL\bar{E}$

Sneutrinos can decay *directly* into pairs of charged leptons, and the “4 Lepton” selection is used to derive exclusion limits, Figure 5(a), for pair produced sneutrinos decaying into the final states $eeee$, $ee\mu\mu$, $ee\tau\tau$, $\mu\mu\mu\mu$, $\mu\mu\tau\tau$ and $\tau\tau\tau\tau$. The different final states correspond to different choices of generation indices. The cross-section limits translate into a lower bound on the muon (tau) sneutrino mass of $M_{\tilde{\nu}_{\mu,\tau}} > 66 \text{ GeV}/c^2$ for the *direct* decays and the worst case coupling.

Indirect decays of sneutrinos are selected using the “4 Leptons + \cancel{E} ” selection. The limits in the $(M_\chi, M_{\tilde{\nu}})$ plane corresponding to this case are shown in Figure 5(b) assuming the $\tilde{\nu}_\mu$ cross-section. Using the bound $M_\chi > 23 \text{ GeV}/c^2$ [5] this limit can be interpreted as $M_{\tilde{\nu}_\mu} > 62 \text{ GeV}/c^2$ for the worst case coupling.

7 Decays via a dominant $LQ\bar{D}$ (λ') Coupling

For a dominant $LQ\bar{D}$ operator the event topologies are mainly characterised by large hadronic activity, possibly with some leptons and/or missing energy. In the simplest case the topology consists of four jet final states, and in the more complicated scenario of multi-jet and multi-lepton and/or multi-neutrino states. The different selections sensitive to the final states expected for this case are summarised in Table 5, and further details can be found in Ref. [6]. For acoplanar jet topologies the AJ-H selection developed for the R-parity conserving SUSY searches are used [23]. The “Multi-jets plus Leptons” and the “2J+2 τ ” selections were updated and reoptimised for the higher centre-of-mass energy as described below.

7.1 Charginos and neutralinos decaying via $LQ\bar{D}$

Three subselections were developed to select the chargino *indirect* topologies [6]. Subselection I is designed to select final states based on the hadronic activity, e.g. $\chi^+\chi^- \rightarrow qq\bar{q}\bar{q} + \chi\chi$; subselection II is designed for decays such as $\chi^+\chi^- \rightarrow l\nu qq + \chi\chi$

where the leptonic energy is more important and subselection III is designed to select the decays $\chi^+\chi^- \rightarrow l\nu l\nu + \chi\chi$. The combination of the three subselections is defined as the “Multi-jets plus Leptons” selection. The complete set of cuts is shown in Table 6. In addition to the variables used for the LLE selections in Section 6.1, the polar angle of the missing energy (Θ_{miss}), the acoplanarity (Φ'_{aco}) and the isolation of the missing momentum vector (E_{10}^{iso}) are used. The prime on a cut variable restricting it to the hadronic system of the event

While the core of the analysis is unchanged with respect to Ref [6], the WW rejection for subselection I, which consists of a two-dimensional cut in the $(M'_{\text{vis}}, \Phi'_{\text{aco}})$ plane, was modified, and the WW rejection for subselections II and III use the quantity χ_{WW}^2 as defined in Equation (2). The selection has lowest efficiencies for final states with taus, which corresponds to the worst case coupling λ'_{3jk} .

A total background of 8.7 events is expected for the inclusive combination of the three subselections, coming dominantly from WW events (7.4 events). In the data 7 events are selected.

Interpreting these results in the framework of the MSSM, 95% C.L. exclusion limits are derived in the (μ, M_2) plane and shown in Figure 2(b) for large scalar masses $m_0 = 500 \text{ GeV}/c^2$. The corresponding lower limit on the mass of the lightest chargino is essentially at the kinematic limit for pair production.

7.2 Squarks decaying via $LQ\bar{D}$

A squark can decay *directly* to a quark and a lepton/neutrino leading to topologies of acoplanar jets and up to two leptons: 2J2L, 2JL ν and 2J2 ν . Couplings with electrons or muons in the final state are neglected as existing limits from the Tevatron [24] exclude the possibility of seeing this signal at LEP. To select $\tilde{q} \rightarrow q\tau$ and $\tilde{q} \rightarrow q\nu$, the “2J+2 τ ” and the “AJ-H” selections are used.

While the core of the “2J+2 τ ” selection is unchanged with respect to Ref. [6], the WW rejection is modified. The quantity χ_{WW}^2 as defined in Equation (2) is required to be $\chi_{WW}^2 > 3.3$. A total of 2.6 events are expected from background processes, which is in good agreement with the observation of 2 events in the data. For the “2J+2 τ ” selection the limit is set by sliding a mass window of width 20 GeV/c^2 centred on the squark mass over the mass spectrum. The resulting squark limits are shown in Figure 6, they correspond to $M_{\tilde{t}_L} > 77 \text{ GeV}/c^2$ assuming $\text{BR}(\tilde{t}_L \rightarrow q\tau) = 100\%$, $M_{\tilde{b}_L} > 80 \text{ GeV}/c^2$ assuming $\text{BR}(\tilde{b}_L \rightarrow q\nu) = 100\%$.

7.3 Sleptons and Sneutrinos decaying via $LQ\bar{D}$

Direct decays of sleptons and sneutrinos via the $LQ\bar{D}$ operator lead to four jet final states. The “Four Jets” selection previously used for the 172 GeV/c^2 $LQ\bar{D}$ analyses is applied [6].

subselection I	subselection II	subselection III
$N_{\text{ch}} \geq 10$ $M_{\text{vis}} > 45 \text{ GeV}/c^2$ $\Theta_{\text{miss}} > 30^\circ$		
$M_{\text{vis}}' > 43\% \sqrt{s}$ $T < 0.9$ $y_5 > 0.003$ $y_6 > 0.002$ $E_T > 60 \text{ GeV}$	$M_{\text{vis}}' < 50\% \sqrt{s}$ $T < 0.74$ $y_4' > 0.0047$ $\left(\begin{array}{c} \Phi'_{\text{aco}} < 145^\circ \\ \text{or} \\ y_6 > 0.002 \end{array} \right)$	$M_{\text{vis}}' < 65 \text{ GeV}/c^2$ $T < 0.8$ $y_4' > 0.001$ $y_6 > 0.00035$
$E_{\text{jet}}^{\text{em}} < 90\% E_{\text{jet}}$ $E_{10}^{\text{iso}} < 5 \text{ GeV}$	$E_{\text{lep}} < 40 \text{ GeV}$ $E_{\text{had}} < 2.5 E_{\text{lep}}$	$E_{\text{had}} < 47\% E_{\text{lep}}$
$\Phi'_{\text{aco}} + 0.55(M_{\text{vis}}' - 120) < 180^\circ$	$\chi_{\text{WW}}^2 > 3.8$	

Table 6: *The list of cuts for the “Multi-jets plus Leptons” selection. Primed event variables are calculated from physical quantities excluding identified leptons.*

After a hadronic final state preselection, the events are forced to four jets and for each of the three possible dijet pairing a 5C-fit (energy-momentum conservation and equal mass constraint) is performed and the pairing with the smallest chisquare is selected. A total of 144 events are observed in the data, in good agreement with the expectation of 142 events. The distribution of the dijet mass ($M_{\text{dijet}}^{\text{5C}}$) for data and Monte Carlo is shown in Figure 7.

Limits are derived by sliding a mass window of $6 \text{ GeV}/c^2$ across the dijet mass distribution, counting the number of events observed and subtracting the expected background according to the prescription given in Ref. [22]. For this purpose the expected background has been assigned a conservative error of 20% [21] and has been reduced by this amount. The results are shown in Figure 8 and imply $M_{\tilde{\nu}_\mu} > 59 \text{ GeV}/c^2$, $M_{\tilde{\mu}_L} > 61 \text{ GeV}/c^2$.

8 Decays via a dominant $\bar{U}\bar{D}\bar{D}$ (λ'') Coupling

For a dominant $\bar{U}\bar{D}\bar{D}$ operator, six jet final states are expected from the pair production of the lightest neutralinos, which subsequently decay to three jets each. The *direct* decays of pair produced right-handed squarks lead to four jet final states. No *direct* decays are possible for sleptons and sneutrinos. The *indirect* chargino decays give rise to a variety of final states depending on the W^* decay, they range from 10 hadronic jets to six jets associated with leptons and missing energy. The *indirect* decays of the squarks lead to eight jet final states. The *indirect* decays of the sleptons lead to six-jets plus two leptons, while the *indirect* decay of the sneutrinos give rise to six-jet final states with missing energy.

A number of new selections, defined in Tables 8-10, have been developed to address the above topologies: “Four Jets Broad”, “Many Jets”, “Many Jets+Leptons”, “Four

Selection	Data	Standard Model Expectation	Direct Decays	Indirect Decays
Four Jets	144	142.0	χ, \tilde{q}	χ^\pm, \tilde{q}
Four Jets Broad	54	48.4		\tilde{q}
Many Jets	1	3.6	χ	χ^\pm
Many Jets+Leptons	1	4.1		χ^\pm
Four Jets+2 Leptons	1	1.1		\tilde{l}
Many Jets+2 Leptons	1	1.2		\tilde{l}
Four Jets+ \cancel{E}	16	18.9		$\tilde{\nu}$
Many Jets+ \cancel{E}	25	26.7		$\tilde{\nu}$

Table 7: *Topologies arising from $\bar{U}\bar{D}\bar{D}$ couplings: the selections, the signal processes giving rise to the above topologies, the number of background events expected, and the number of candidate events selected in the data, quoted with any sliding mass cuts removed.*

Jets+2 Leptons”, “Many Jets+2 Leptons”, “Four Jets+ \cancel{E} ” and Many Jets+ \cancel{E} . In addition the “Four Jets” selection of Section 7.3 is also utilised. In order for the selections to be applicable for any choice of couplings, b -tagging requirements are not applied.

These selections rely mainly on two characteristics of the events; mass reconstruction of the pair produced sparticles and/or the presence of many jets in the event. Monte Carlo studies of these many jet topologies show that when the boost of the sparticles is high (i.e. far from threshold) the jets in each hemisphere become merged and the event can be considered as ‘four jet like’. In this boosted regime, adequate mass resolution on a pair of equal mass sparticles is obtained using the “Four Jet” selection (Section 7.3). For example, Figures 9(a)-(d) show the distribution of reconstructed dijet mass (M_{dijet}^{5C}) obtained for a pair of 50 GeV/ c^2 sparticles decaying to 6 q (*direct* neutralino), 8 q (*indirect* squarks), 6 q 2 l (*indirect* slepton) and 10 q (*indirect* chargino) topologies. The Gaussian core of the dijet mass distribution ranges from ≈ 1.8 GeV/ c^2 for the six quark events to ≈ 2.6 GeV/ c^2 for the ten quark events. The mass resolution is only weakly dependent on the choice of the λ''_{ijk} coupling; the worst dijet mass resolution corresponding to a λ''_{223} . For *indirect* decays, in addition to the dependence on the jet multiplicity, the mass resolution is also sensitive to the mass of the neutralino involved in the decay. For sparticle masses closer to threshold, the jets from each sparticle are less clearly separated and the mass reconstruction deteriorates significantly. In this regime selections based on requiring a large Durham distance are employed.

Table 7 gives a list of all the selections, the signal processes addressed by the selections, and the number of observed and expected events. The selections are described in detail in the following Sections 8.1-8.4.

8.1 Charginos and neutralinos decaying via $\bar{U}\bar{D}\bar{D}$

From the pair production of the lightest neutralino six jet topologies are expected. The “Many Jets” selection is used for neutralino masses $M_\chi > 60 \text{ GeV}/c^2$, and the “Four Jets” selection for $M_\chi < 60 \text{ GeV}/c^2$. The selection efficiency varies between 10%–20% depending on the mass.

The “Many Jets” selection (Table 8) is needed when the boost in the event is small and the mass resolution deteriorates. For this selection no attempt is made to reconstruct the sparticle masses, instead events with many jets are selected by requiring the Durham distance for the transition between five to six jets (y_6) to be large. The distribution of this variable for the background and an example signal is shown in Figure 10. A value of y_6 greater than 0.006 is required. To remove hadronic W decays, events for which the dijet mass is around the W mass are rejected. A total of 3.6 background events are predicted from the Monte Carlo simulation, 1 event is observed in the data.

For the *indirect* chargino decays, which can have leptons in the final state, the “Many Jets+Lepton” selection (Table 8) is used in addition to the “Four Jets” and “Many Jets” selections. For the “Many Jets+Lepton” selection, after a preselection, at least one lepton with energy (E_{lep}) between 3 GeV and 20 GeV is required. The cut on y_6 is looser compared to the “Many Jets” selection, while the hadronic W background is reduced using the same cuts as used in the “Many Jets” selection. The efficiencies are generally higher for the *indirect* chargino decays than for the *direct* neutralino decays as the larger number of jets leads to a higher y_6 .

Interpreting these results in the framework of the MSSM, Figure 2(c) shows the 95% C.L. exclusion in the (μ, M_2) plane obtained assuming $m_0 = 500 \text{ GeV}/c^2$. As for the λ and λ' couplings the lower limit on the chargino mass is essentially at the kinematic limit.

8.2 Squarks decaying via $\bar{U}\bar{D}\bar{D}$

The *direct* decay of pair produced squarks leads to four quark final states. The “Four Jets” selection is therefore used to extract the mass limits. As shown in Figure 8 the mass limits are $69 \text{ GeV}/c^2$ for scalar up type squarks and $49 \text{ GeV}/c^2$ for scalar down type squarks.

For the *indirect* squark decays, which lead to eight jet topologies a slightly modified “Four Jets” selection is used in addition to the “Four Jets” selection. This “Four Jets Broad” selection (Table 8) uses a looser sliding mass window cut, as the mass resolution on the dijet masses is degraded compared to that obtained for the *direct* squark decays. The increased number of jets also allows a tighter cut on y_6 . The efficiencies are typically around 10%. The 95% C.L. exclusion in the $(M_\chi, M_{\bar{q}})$ plane for a left-handed stop and left-handed sbottom are shown in Figure 11, the corresponding mass limits are $M_{\bar{t}_L} > 58 \text{ GeV}/c^2$ and $M_{\bar{b}_L} > 57 \text{ GeV}/c^2$ for $M_\chi > 20 \text{ GeV}/c^2$.

Four Jets Broad	Many Jets	Many Jets + Leptons
$N_{\text{ch}} > 8, T < 0.9$ $ p_z^{\text{miss}} < 1.5(M_{\text{vis}} - 90), p_z^{\text{miss}} /p^{\text{miss}} < 0.95$ $E_{\text{jet}}^{\text{em}} < 95\%E_{\text{jet}}$		
$E_{\text{vis}}/\sqrt{s} > 0.7$	$E_{\text{vis}}/\sqrt{s} > 0.7$	$E_{\text{vis}}/\sqrt{s} < 0.95$ $N_{\text{lep}} \geq 1$ $3 < E_{\text{lep}} < 20 \text{ GeV}$
$y_4 > 0.006$ $y_6 > 0.0015$	$y_5 > 0.01$ $y_6 > 0.006$	$y_6 > 0.0025$
$ M_{12} - M_{34} < 12 \text{ GeV}/c^2$ $ M_{\text{dijet}}^{5C} - M_\chi < 2.5 \text{ GeV}/c^2$	$ M_{\text{dijet}}^{5C} - M_W > 2.5 \text{ GeV}/c^2$	$ M_{\text{dijet}}^{5C} - M_W > 2.5 \text{ GeV}/c^2$

Table 8: *The list of cuts for the “Four Jets Broad”, “Many Jets” and “Many Jets+Leptons” selections. These selections are used for chargino, neutralino and indirect squark decays via an $\bar{U}DD$ operator.*

Four Jets + 2 Leptons	Many Jets + 2 Leptons
$N_{\text{ch}} > 8, 0.5 < T < 0.95$ $ p_z^{\text{miss}} < 1.5(M_{\text{vis}} - 90), p_z^{\text{miss}} /p^{\text{miss}} < 0.95$ $E_{\text{jet}}^{\text{em}} < 95\%E_{\text{jet}}$ $E_{\text{vis}}/\sqrt{s} > 0.8, E_T > 45 \text{ GeV}$ $N_{\text{lep}} \geq 2$ (same flavour, opposite charge)	
$E_{\text{lep}} > 10 \text{ GeV}$	$E_{\text{lep}} > 5 \text{ GeV}$
$y_4 > 0.0005$	$y_6 > 0.0012$
$ M_{12} - M_{34} < 10 \text{ GeV}/c^2$ $ M_{\text{dijet}}^{5C} - M_{\tilde{\ell}} < 5 \text{ GeV}/c^2$	$ M_{\text{dijet}}^{5C} - M_W > 3 \text{ GeV}/c^2$

Table 9: *The list of cuts for the “Four Jets + 2 Leptons” and “Many Jets + 2 Leptons” selections, as used for the indirect slepton searches decaying via an $\bar{U}DD$ operator.*

Four Jets + \cancel{E}	Many Jets + \cancel{E}
$N_{\text{ch}} > 8$ $ p_z^{\text{miss}} /p^{\text{miss}} < 0.95$ $E_{\text{jet}}^{\text{em}} < 95\%E_{\text{jet}}, E_T > 45 \text{ GeV}, E_{\text{lep}} < 15 \text{ GeV}$	
$0.25 < E_{\text{vis}}/\sqrt{s} < 0.75$ $\Delta\phi_T < 160^\circ, E_t > 45 \text{ GeV}$ $0.5 < T < 0.97$	$0.7 < E_{\text{vis}}/\sqrt{s} < 0.95$ $0.6 < T < 0.97$
$y_4 > 0.001$ $y_6 > 0.0003$	$y_4 > 0.005$ $y_6 > 0.002$ (0.005 if $M(\chi) > 60 \text{ GeV}$)
$ M_{12} - M_{34} < 10 \text{ GeV}/c^2$ $ M_{12} + M_{34} - 2M_\chi < M_\chi/3$	if $M(\chi) < 60 \text{ GeV}/c^2$: $ M_{12} - M_{34} < 10 \text{ GeV}/c^2$ if $M(\chi) < 60 \text{ GeV}/c^2$: $ M_{12} + M_{34} - 2M_\chi < M_\chi/3$

Table 10: *The list of cuts for the “Four Jets + \cancel{E} ” and “Many Jets + \cancel{E} ” selections, as used for the indirect sneutrino searches via an $\bar{U}\bar{D}\bar{D}$ operator.*

8.3 Sleptons decaying via $\bar{U}\bar{D}\bar{D}$

No *direct* slepton decays are possible via the λ'' coupling. For the *indirect* decays of selectron and smuon pairs, the “Four Jets + 2 Leptons” is used for large mass differences between the slepton and neutralino, and the “Many Jets + 2 Leptons” for the low mass difference region. The efficiencies are typically between 50-60%.

For the “Four Jets + 2 Leptons” selection (Table 9), at least two identified leptons above 10 GeV are required, with the two most energetic leptons required to be of the same flavour and opposite charge. A loose sliding cut on the dijet mass is also used.

For the “Many Jets + 2 Leptons” selection (Table 9), requirements on y_6 are combined with requirements on the presence of at least two identified leptons above 5 GeV, with the two most energetic required to be of same flavour and opposite charge.

Figure 12 shows the 95% C.L. exclusion in the $(M_\chi, M_{\tilde{\ell}})$ plane for selectrons and smuons. The selectron cross-section is evaluated in the gaugino region ($\mu = -200 \text{ GeV}/c^2$, $\tan\beta = 2$) where constructive neutralino t-channel interference enhances the cross-section. The shape of the limits at $M_\chi \approx 20 \text{ GeV}/c^2$ is due to the switch between selections. The non-excluded region at very small mass differences between the slepton and the neutralino is because the lepton is very soft and the selection efficiency drops to zero. For $M_{\tilde{\ell}} - M_\chi > 10 \text{ GeV}/c^2$ the excluded masses are: $M_{\tilde{e}_R}(M_{\tilde{e}_L}) > 81(70) \text{ GeV}/c^2$ and $M_{\tilde{\mu}_R}(M_{\tilde{\mu}_L}) > 67(70) \text{ GeV}/c^2$.

8.4 Sneutrinos decaying via $\bar{U}\bar{D}\bar{D}$

No *direct* sneutrino decays are possible via the λ'' coupling. Sneutrinos decaying *indirectly* lead to final states containing two neutrinos. Large mass differences between the sneutrino and neutralino lead to event topologies with significant missing energy, and the “Four Jets + \cancel{E} ” is used. For small mass differences the “Many Jets + \cancel{E} ” selection is used. The efficiencies range from 10-40% depending on the sneutrino and neutralino masses involved.

For the “Four Jets + \cancel{E} ” selection (Table 10) large missing energy is required and events with energetic leptons are vetoed. Due to the presence of the neutrinos, the 5C mass fit is no longer useful (Figure 9(e)). Nevertheless the resolution on the dijet masses (M_{12} and M_{34}) before the 5C fit is sufficient to allow reconstruction of the neutralino mass (rather than the sneutrino mass) for many choices of sneutrino/neutralino masses (e.g. Figure 9(f)). As the mass resolution is found to depend on the neutralino mass involved in the decay, the width of the sliding mass window is a function of the assumed neutralino mass.

The “Many Jets + \cancel{E} ” selection is summarised in Table 10. Compared to the “Four Jets + \cancel{E} ” selection, the more spherical topology of the sneutrino decays close to threshold is used in the following way: For neutralino masses above 60 GeV a $y_6 > 0.05$ is required. For neutralino masses below 60 GeV a looser $y_6 > 0.002$ is used, reinforced by the same sliding mass window cut on the dijet mass as applied for the “Four Jets + \cancel{E} ” selection.

Figure 13(a) shows the 95% C.L. exclusion in the $(M_\chi, M_{\tilde{\nu}})$ plane for the electron

sneutrino. The cross-section is evaluated in the gaugino region, where it is enhanced by constructive chargino t-channel interference. The limit $M_{\tilde{\nu}_e} > 70 \text{ GeV}/c^2$ is obtained. In Figure 13(b) the exclusion obtained assuming three mass degenerate sneutrinos is also presented, with cross-sections evaluated in a region where the t-channel enhancement in the $\tilde{\nu}_e$ cross-section is negligible.

9 Conclusions

A number of search analyses have been developed to select R-parity violating SUSY topologies from the pair-production of sparticles. It was assumed that the LSP has a negligible lifetime, and that only one coupling λ_{ijk} , λ'_{ijk} or λ''_{ijk} is non-zero. The search analyses for the various topologies yield good agreement between the number of observed and expected events, thus there is no evidence for R-parity violating supersymmetry in the data collected at $\sqrt{s} = 181\text{--}184 \text{ GeV}$. Lower limits on the masses of various sparticles are set within the framework of the MSSM.

For large m_0 the chargino mass limit is given by the kinematic limit $M_\chi > 91 \text{ GeV}/c^2$, irrespective of the R-parity violating operator.

The limits for *direct* decays of sleptons for an $LL\bar{E}$ coupling are $M_{\tilde{e}_R} > 82 \text{ GeV}/c^2$ in the gaugino region ($\mu = -200 \text{ GeV}/c^2$, $\tan\beta = 2$), $M_{\tilde{\mu}_R} > 61 \text{ GeV}/c^2$ and $M_{\tilde{\nu}_\mu} > 66 \text{ GeV}/c^2$. The limits for the *direct* decays of sleptons and squarks in the case of an $LQ\bar{D}$ coupling are $M_{\tilde{\mu}_L} > 61 \text{ GeV}/c^2$, $M_{\tilde{\nu}_\mu} > 59 \text{ GeV}/c^2$ and $M_{\tilde{t}_L} > 77 \text{ GeV}/c^2$ for $\text{Br}(\tilde{t}_L \rightarrow q\tau) = 1$. The limit for squarks assuming an $\bar{U}\bar{D}\bar{D}$ coupling are $M_{\tilde{u}_R} > 69 \text{ GeV}/c^2$ and $M_{\tilde{d}_R} > 49 \text{ GeV}/c^2$.

For the *indirect* decays of sfermions, the following limits have been obtained, derived in the gaugino region ($\mu = -200 \text{ GeV}/c^2$, $\tan\beta = 2$) for \tilde{e} and $\tilde{\nu}_e$.

- $M_{\tilde{t}_L} > 61 \text{ GeV}/c^2$ for $LL\bar{E}$ and $58 \text{ GeV}/c^2$ for $\bar{U}\bar{D}\bar{D}$ ($M_\chi > 20 \text{ GeV}/c^2$)
- $M_{\tilde{e}_R} > 76 \text{ GeV}/c^2$ for $LL\bar{E}$ and $81 \text{ GeV}/c^2$ for $\bar{U}\bar{D}\bar{D}$ ($M_{\tilde{e}_R} - M_\chi > 10 \text{ GeV}/c^2$)
- $M_{\tilde{\mu}_R} > 74 \text{ GeV}/c^2$ for $LL\bar{E}$ and $67 \text{ GeV}/c^2$ for $\bar{U}\bar{D}\bar{D}$ ($M_{\tilde{\mu}_R} - M_\chi > 10 \text{ GeV}/c^2$)
- $M_{\tilde{\tau}_R} > 70 \text{ GeV}/c^2$ for $LL\bar{E}$
- $M_{\tilde{\nu}} > 62 \text{ GeV}/c^2$ for $LL\bar{E}$
- $M_{\tilde{\nu}_e} > 70 \text{ GeV}/c^2$ for $\bar{U}\bar{D}\bar{D}$

These mass limits represent significant improvements over those previously published [5, 6, 8].

10 Acknowledgements

It is a pleasure to congratulate our colleagues from the accelerator divisions for the successful operation of LEP at high energy. We would like to express our gratitude to the engineers and support people at our home institutes without whose dedicated help this work would not have been possible. Those of us from non-member states wish to thank CERN for its hospitality and support.

References

- [1] For a review see for example H.P. Nilles, Phys. Rep. **110** (1984) 1; H. E. Haber and G. L. Kane, Phys. Rep. **117** (1985) 75.
- [2] G. Farrar and P. Fayet, Phys. Lett. **B 76** (1978) 575.
- [3] S. Weinberg, Phys. Rev. **D 26** (1982) 287; N. Sakai and T. Yanagida Nucl. Phys. **B 197** (1982) 83; S. Dimopoulos, S. Raby and F. Wilczek, Phys. Lett. **B 212** (1982) 133.
- [4] L. J. Hall and M. Suzuki, Nucl. Phys. **B 231** (1984) 419; D. E. Brahm, L. J. Hall, Phys. Rev. **D 40** (1989) 2449; . E. Ibanez, G. G. Ross, Nucl. Phys. **B 368** (1992) 3; A. Chamseddine and H. Dreiner, Nucl. Phys. **B 458** (1996) 65; A. Yu. Smirnov, F. Vissani, Nucl. Phys. **B 460** (1996) 37.
- [5] ALEPH Collaboration, “*Search for supersymmetry with a dominant R-Parity violating $LL\bar{E}$ Coupling in e^+e^- Collisions at centre-of-mass energies of 130 GeV to 172 GeV*”, Eur. Phys. J. **C 4**, 433-451 (1998).
- [6] ALEPH Collaboration, “*Search for supersymmetry with a dominant R-Parity violating $LQ\bar{D}$ Coupling in e^+e^- Collisions at centre-of-mass energies of 130 GeV to 172 GeV*”, CERN EP/98-147, accepted by Eur. Phys. J. C.
- [7] ALEPH Collaboration, “*Search for supersymmetric particles with R-parity violation in Z decays*”, Phys. Letts. **B 349** (1995) 238.
- [8] OPAL Collaboration, “*Searches for R-Parity Violating Decays of Gauginos at 183 GeV at LEP*”, CERN-EP/98-203, submitted to Eur. Phys. J. C.
- [9] G. Bhattacharyya, hep-ph/9709395; G. Bhattacharyya, Nucl. Phys. Proc. Suppl. **52A** (1997) 83.
- [10] ALEPH Collaboration, “*ALEPH: a detector for electron-positron annihilations at LEP*”, Nucl. Instr. Meth. **A 294** (1990) 121.
- [11] ALEPH Collaboration, “*Performance of the ALEPH detector at LEP*”, Nucl. Instr. Meth. **A 360** (1995) 481.

- [12] S. Katsanevas and P. Morawitz, “*SUSYGEN 2.2 – A Monte Carlo event generator for MSSM Sparticle production at e^+e^- Colliders*”, Comp. Phys. Comm. **(112)2-3** (1998) 227.
- [13] ALEPH Collaboration, “*Searches for scalar top and scalar bottom quarks at LEP2*”, Phys. Lett. **B 413** (1997) 431.
- [14] T. Sjöstrand, “*The PYTHIA 5.7 and JETSET 7.4 manual*”, LU-TP 95/20, CERN-TH 7112/93, Comp. Phys. Comm. **82** (1994) 74.
- [15] M. Skrzypek, S. Jadach, W. Placzek and Z. Wąs, Comp. Phys. Comm. **94** (1996) 216.
- [16] H. Anlauf et al., Comp. Phys. Comm. **79** (1994) 466.
- [17] S. Jadach, B. F. L. Ward and Z. Was, Comp. Phys. Comm. **79** (1994) 503.
- [18] J.A.M. Vermaseren in “*Proceedings of the IVth international Workshop on Gamma Gamma Interactions*”, Eds. G. Cochar and P. Kessler, Springer Verlag, 1980.
- [19] J. -F. Grivaz and F. Le Diberder, “*Complementary analyses and acceptance optimization in new particle searches*”, LAL preprint # 92-37 (1992).
- [20] ALEPH Collaboration, “*Search for sleptons in e^+e^- collisions at centre-of-mass energies up to 184 GeV*”, Phys. Lett. **B 433**, (1998) 176.
- [21] ALEPH Collaboration, “*Search for charged Higgs bosons in e^+e^- collisions at centre-of-mass energies from 130 to 172 GeV*”, Phys. Lett. **B 418** (1998) 419.
- [22] R. M. Barnett et al., Phys. Rev. **D 54** (1996) 1.
- [23] ALEPH Collaboration, “*Searches for Charginos and Neutralinos in e^+e^- collisions at centre of mass energies near 183 GeV and constraints on the MSSM parameter space*”, CERN EP/99-014, submitted to Euro. Phys. J. C.;
ALEPH Collaboration, “*Searches for Charginos and Neutralinos in e^+e^- collisions at $\sqrt{s} = 161$ and 172 GeV*”, Eur. Phys. J. **C 2** (1998) 417.
- [24] CDF Collaboration, “*Search for Leptoquarks at CDF*”, proceedings of HEP 97, Stonybrook; D0 Collaboration, “*D0 Search for Leptoquarks*”, *ibid*;
CDF Collaboration, “*Search for first generation Leptoquark pair production in $p\bar{p}$ collisions at $\sqrt{s} = 1.8$ TeV*”, Phys. Rev. Lett. **79**, 4327 (1997);
CDF Collaboration, “*Search for second generation Leptoquarks in the dimuon plus dijet channel of $p\bar{p}$ collisions at $\sqrt{s} = 1.8$ TeV*”, FERMILAB-PUB-98/219-E, submitted to Phys. Rev. Lett.

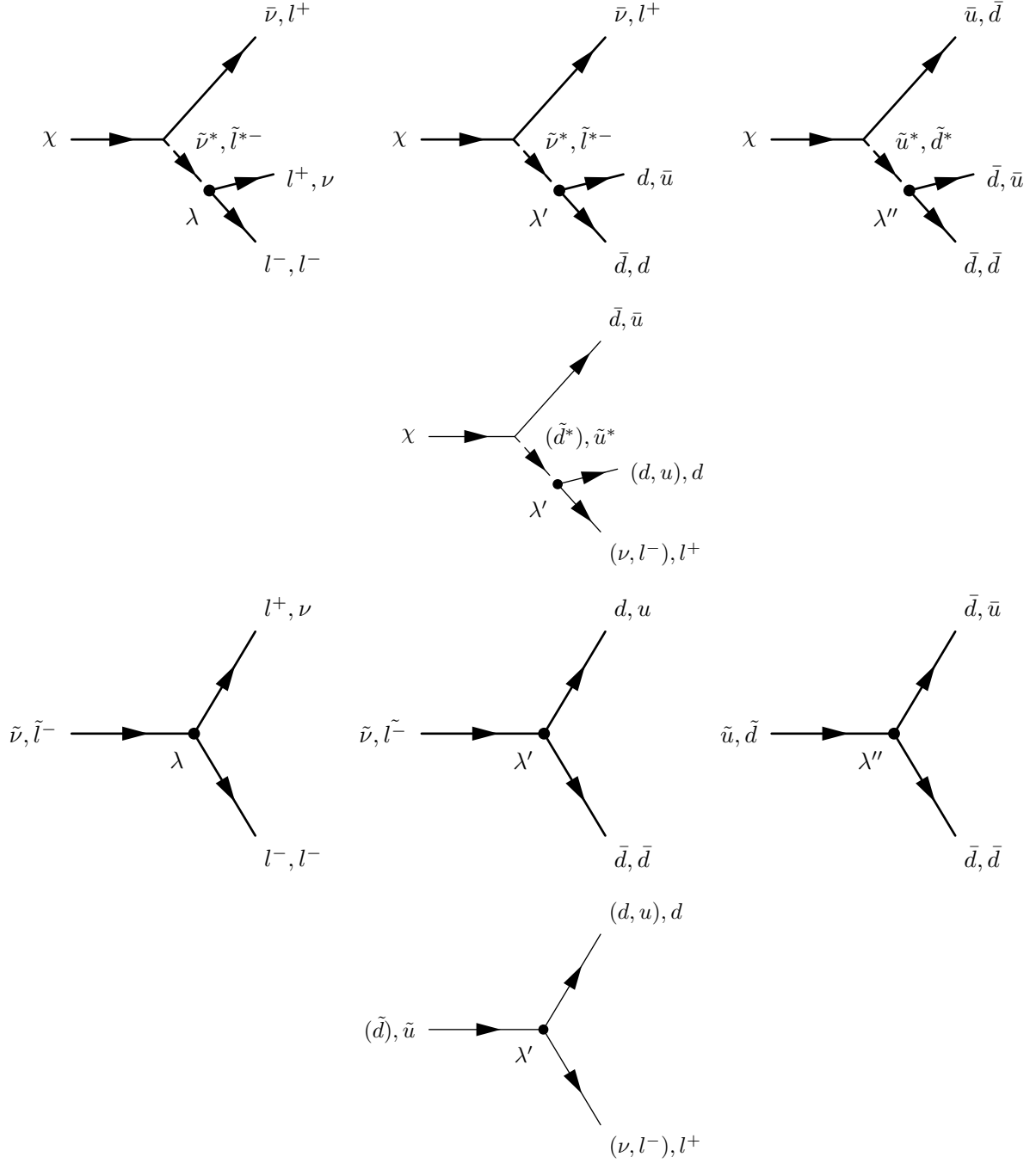


Figure 1: Direct R -parity violating decays of supersymmetric particles via the λ , λ' and λ'' couplings. The black dot marks the R -parity violating vertex in the decay.

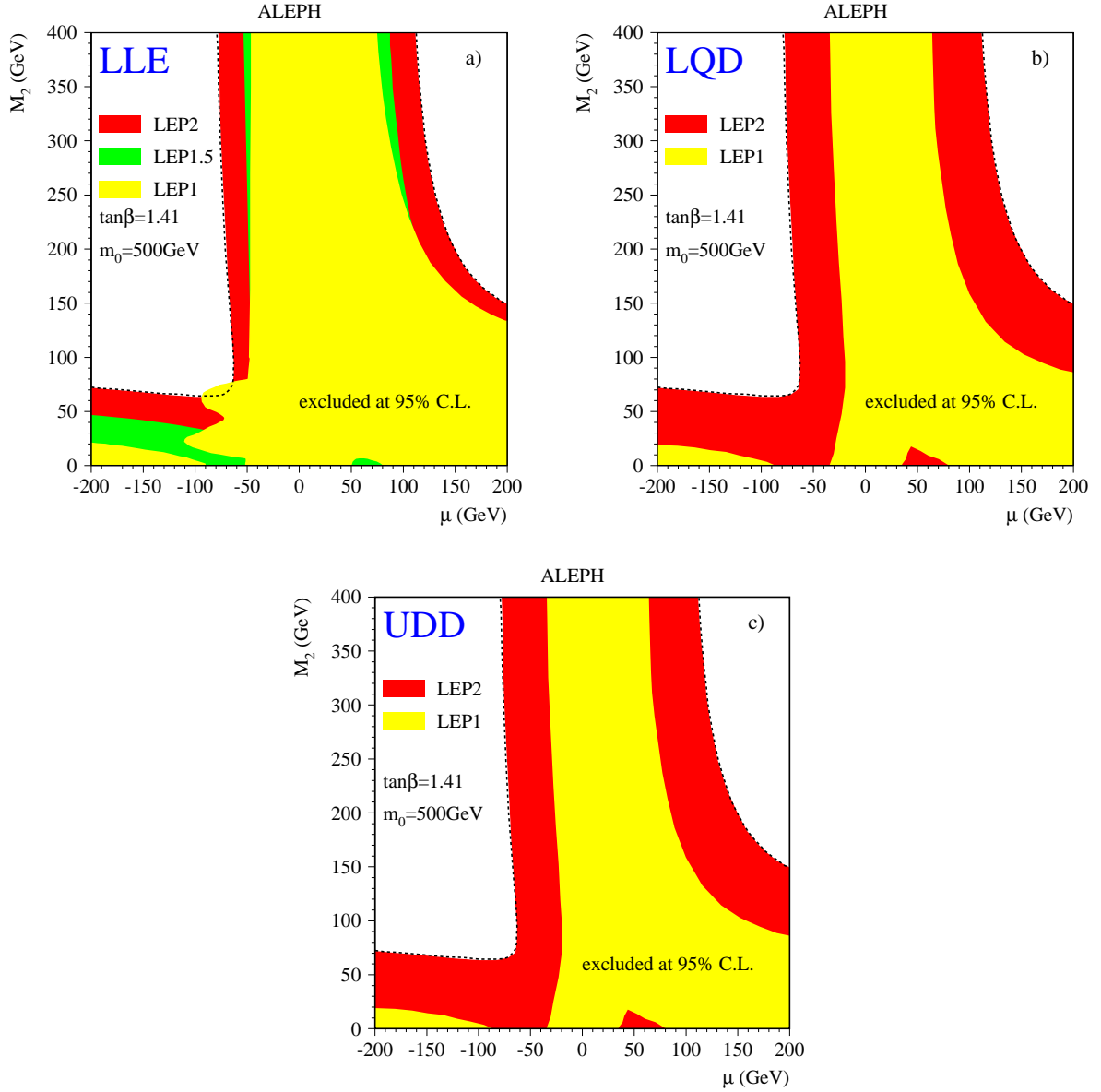


Figure 2: *Regions in the (μ, M_2) plane excluded at 95% C.L. at $\tan\beta = 1.41$ and $m_0 = 500 \text{ GeV}/c^2$ for the three operators. The dotted line is the kinematic limit for the pair production of the lightest chargino.*

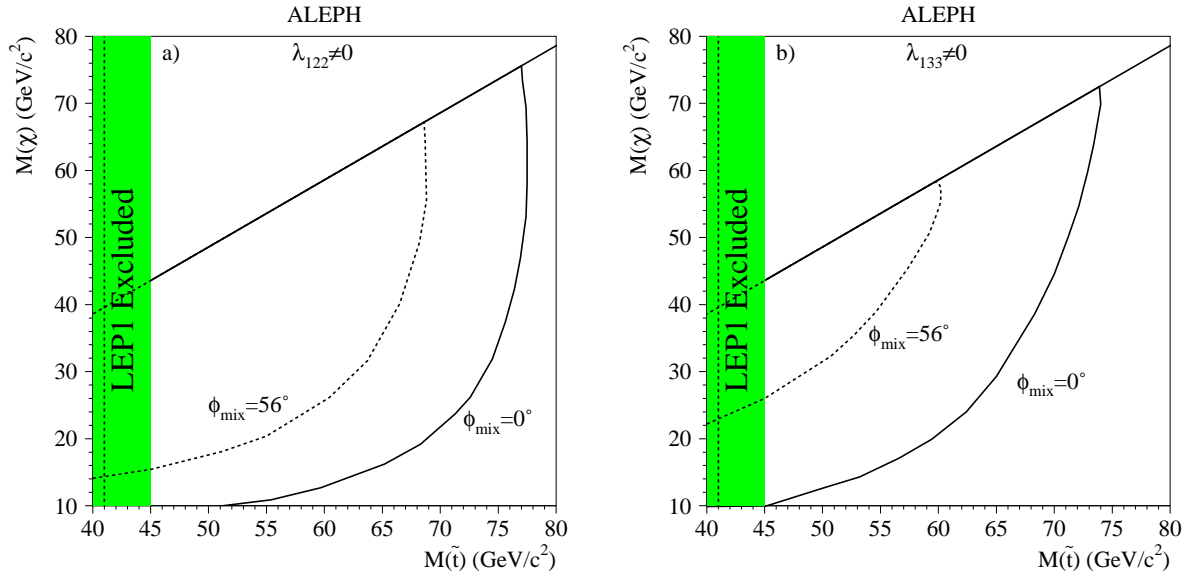


Figure 3: The 95% C.L. limits in the $(M_\chi, M_{\tilde{t}})$ plane for indirect stop decays via a $LL\bar{E}$ couplings a) λ_{122} and b) λ_{133} . The two mixing angles chosen correspond to the best and worst case cross-sections. The LEP 1 limit for $\phi_{\text{mix}} = 0^\circ$ (and $\phi_{\text{mix}} = 56^\circ$ -dashed line) is also shown.

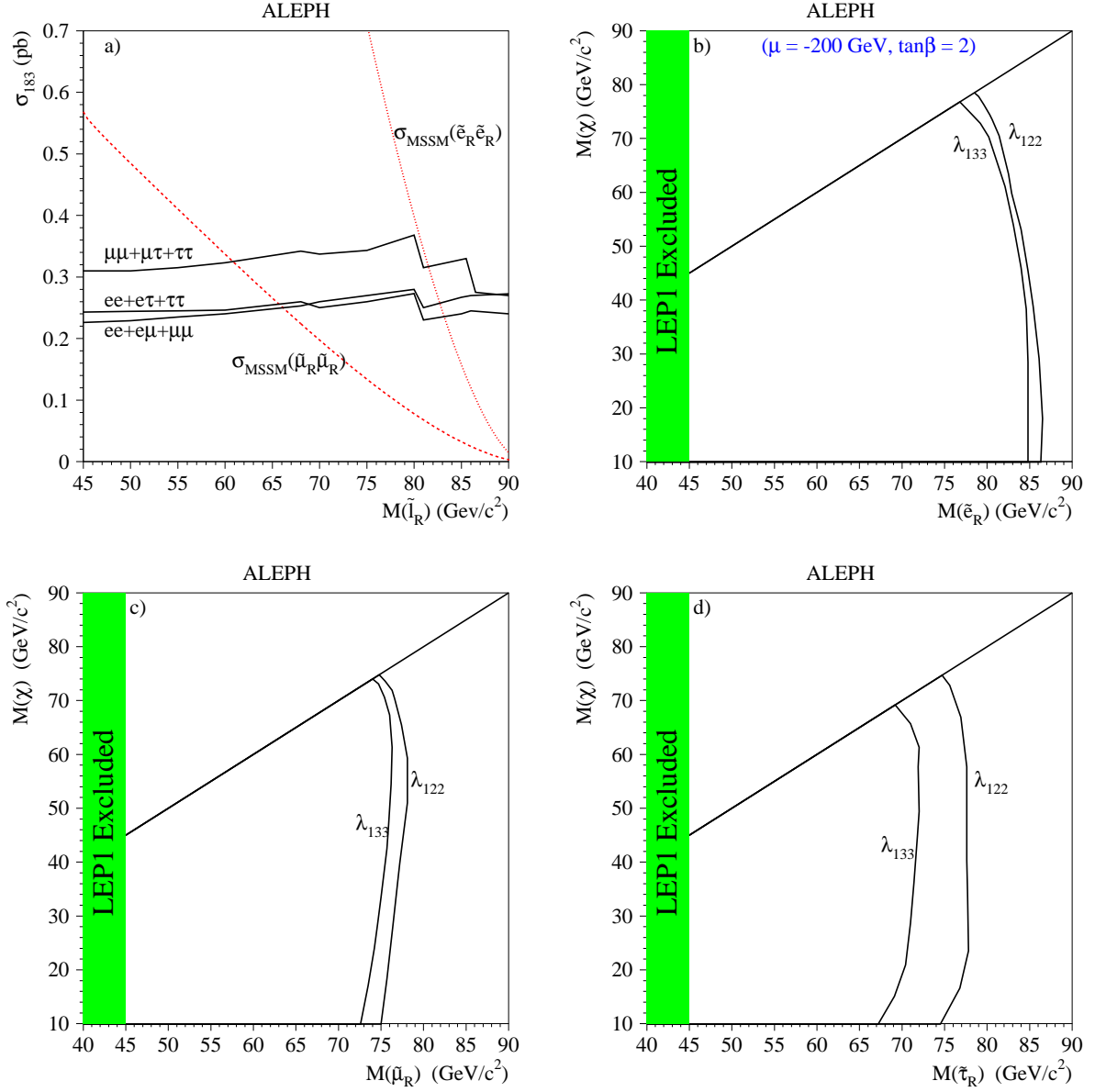


Figure 4: a) The 95% C.L. exclusion cross-sections scaled to $\sqrt{s} = 183 \text{ GeV}$ for sleptons decaying directly via a dominant $LL\bar{E}$ operator. For the purpose of this plot a β^3/s cross-section dependence was assumed. The dashed line shows the MSSM cross-section for pair production of right-handed smuons, the dashed-dotted the cross-section for right-handed selectrons at $\tan\beta = 2, \mu = -200 \text{ GeV}/c^2, M_2 = 50 \text{ GeV}/c^2$. Figs b), c) and d) show the 95% C.L. limits in the $(M_\chi, M_{\tilde{l}})$ plane for selectrons, smuons and staus decaying indirectly via a dominant $LL\bar{E}$ operator. The two choices of λ_{122} and λ_{133} correspond to the best and worst case exclusions respectively. The selectron cross-section is evaluated in the gaugino region at $\mu = -200 \text{ GeV}/c^2, \tan\beta = 2$.

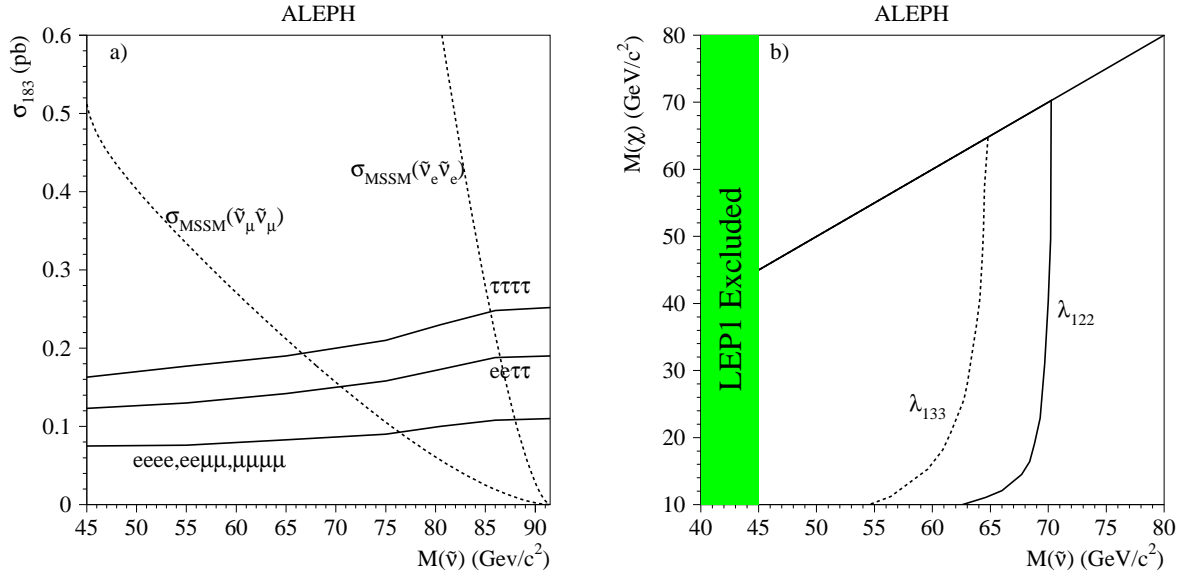


Figure 5: a) The 95% C.L. exclusion cross-sections scaled to $\sqrt{s} = 183$ GeV for sneutrinos decaying directly via a dominant $LL\bar{E}$ operator. For the purpose of this plot a β^3/s cross-section dependence was assumed. The MSSM cross-sections ($\tan\beta = 2$) for pair production of electron sneutrinos ($\mu = -200$ GeV/c², $M_2 = 100$ GeV/c²) and muon sneutrinos are superimposed. b) The 95% C.L. limits in the $(M_\chi, M_{\tilde{\nu}})$ plane valid for indirect $\tilde{\nu}_\mu$ and $\tilde{\nu}_\tau$ decays. The limits for $\tilde{\nu}_e$ are always at least as stringent as those presented. The two choices of λ_{122} and λ_{133} correspond to the best and worst case exclusions respectively.

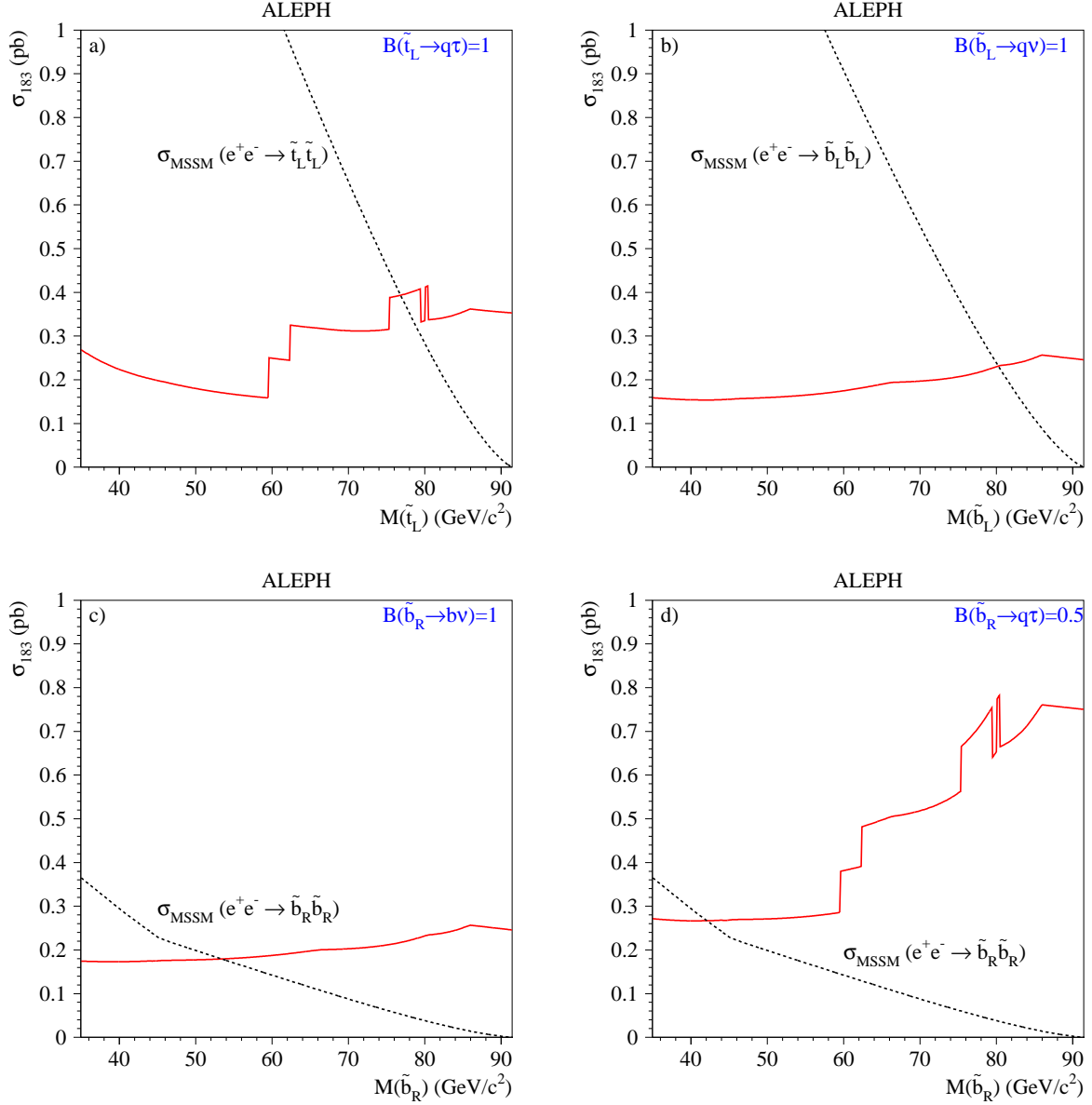


Figure 6: The 95% C.L. excluded cross sections for the direct squark decays via a dominant $LQ\bar{D}$ operator: a) $\tilde{t}_L\tilde{t}_L \rightarrow \tau q\tau q$, b) $\tilde{b}_L\tilde{b}_L \rightarrow q\nu q\nu$, c) $\tilde{b}_R\tilde{b}_R \rightarrow b\nu b\nu$ and d) \tilde{b}_R production with a 50% branching ratio into $q\tau$ and $q\nu$. The MSSM cross sections are superposed as dashed lines.

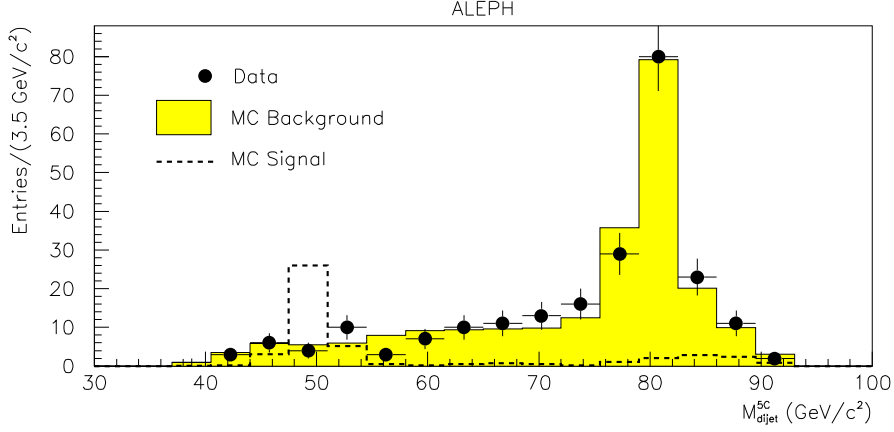


Figure 7: *Data/Monte Carlo comparison of the reconstructed dijet mass after forcing the event to four jets and performing the 5C fit. The dashed line is the signal for 50 GeV/c² left-handed selectrons decaying directly via the $LQ\bar{D}$ coupling, normalised to a cross-section of 2.4 pb.*

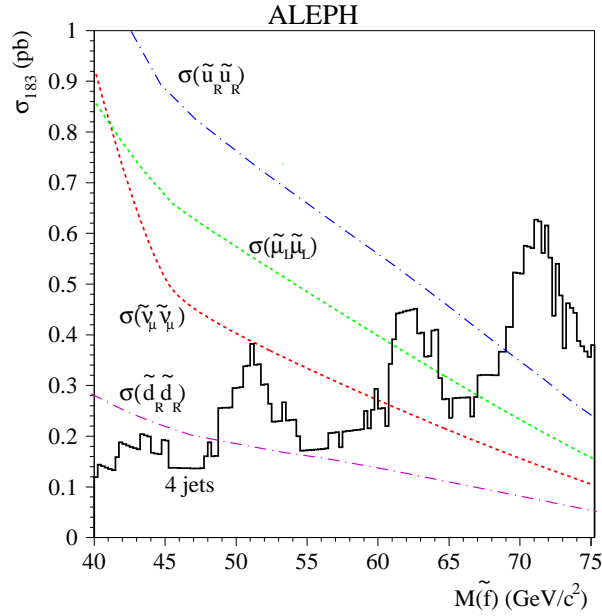


Figure 8: *The 95% C.L. excluded cross-sections scaled to $\sqrt{s} = 183$ GeV for sleptons (via $LQ\bar{D}$), sneutrinos (via $LQ\bar{D}$) and squarks (via $\bar{U}D\bar{D}$) decaying directly to four jets. The MSSM cross-sections for pair production of muon sneutrinos, left-handed smuons and right-handed squarks are superimposed.*

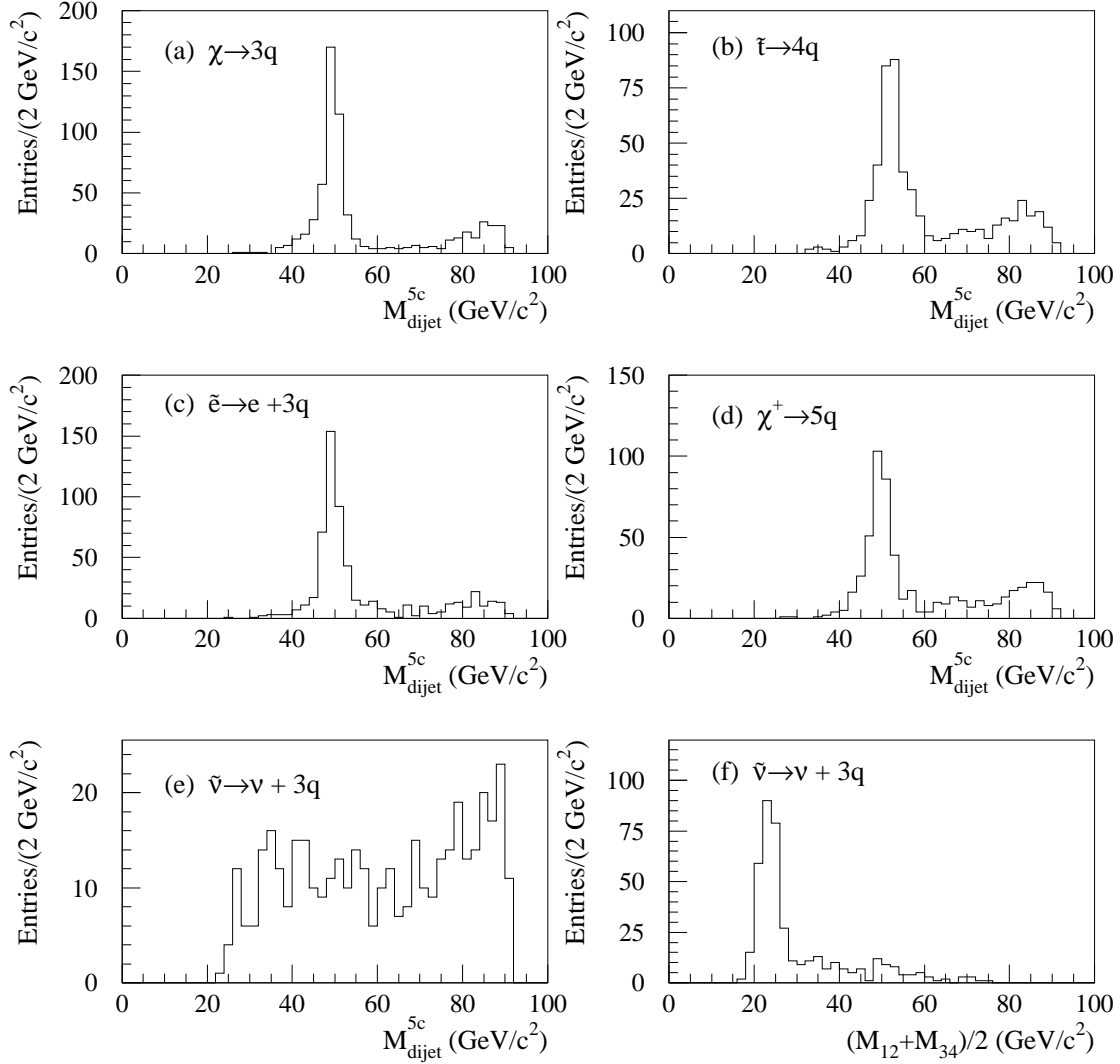


Figure 9: Mass reconstruction for various $\bar{U}\bar{D}\bar{D}$ decay topologies: Dijet mass distribution of events (forced to 4 jets), after the 5C fit, for boosted pairs of sparticles ($M_{\tilde{f}} = 50 \text{ GeV}/c^2$, $M_{\chi} = 25 \text{ GeV}/c^2$). (a) 6 quarks, (b) 8 quarks, (c) 6 quarks + 2 leptons, (d) 10 quarks, (e) 6 quarks + 2 ν . As can be seen from (e), in the presence of missing energy the mass reconstruction for the sneutrino, using the 5C fit, no longer works. For this case, using the sum of dijet masses before the 5C fit (f) allows reconstruction of the χ mass instead.

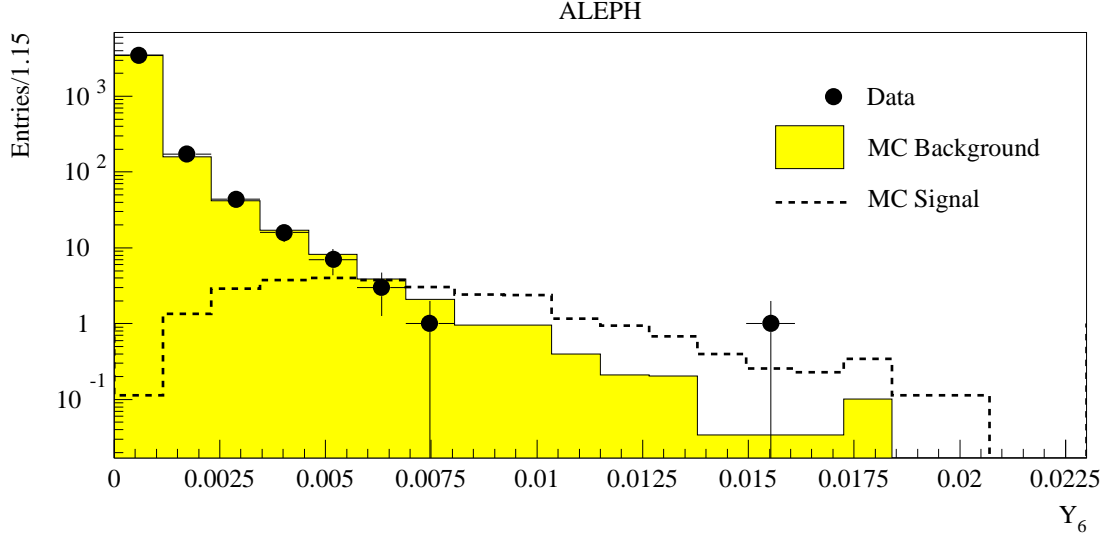


Figure 10: *Data/Monte Carlo comparison of the Durham y_6 distance. The dashed line is the expected signal for $\chi^+\chi^-$ ($M_{\chi^+} = 90 \text{ GeV}/c^2$) decaying indirectly via a $\bar{U}\bar{D}\bar{D}$ operator to χ ($M_\chi = 40 \text{ GeV}/c^2$), assuming a production cross-section of 0.5 pb .*

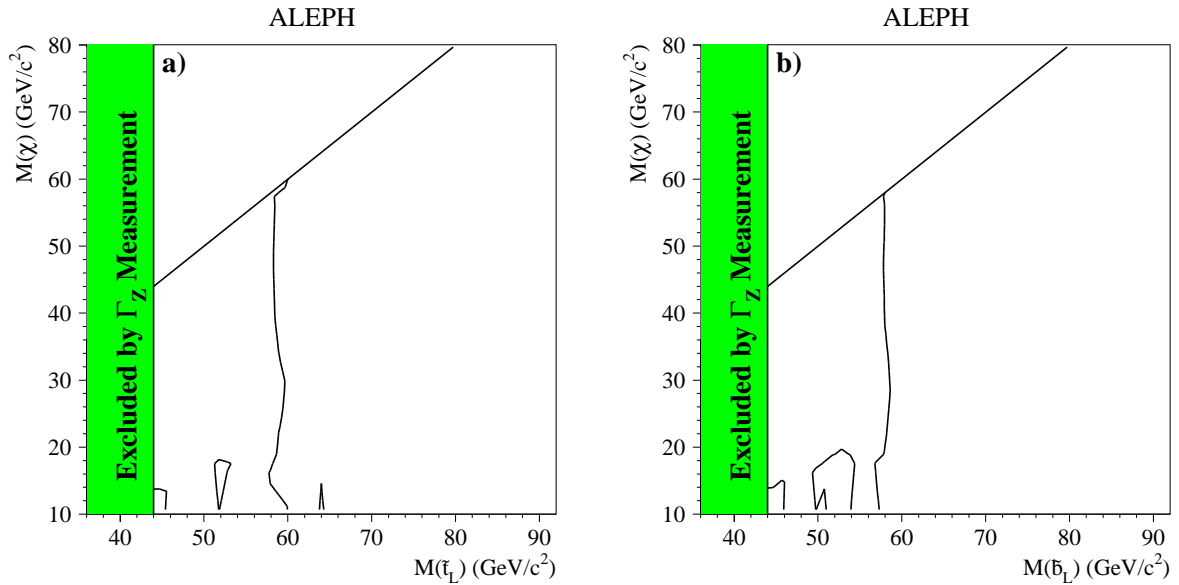


Figure 11: *The 95% C.L. exclusion for squarks decaying indirectly via a dominant $\bar{U}\bar{D}\bar{D}$ operator: (a) left-handed stop, (b) left-hand sbottom. (The non-excluded regions for neutralino masses less than $20 \text{ GeV}/c^2$ are excluded at 90% C.L.).*

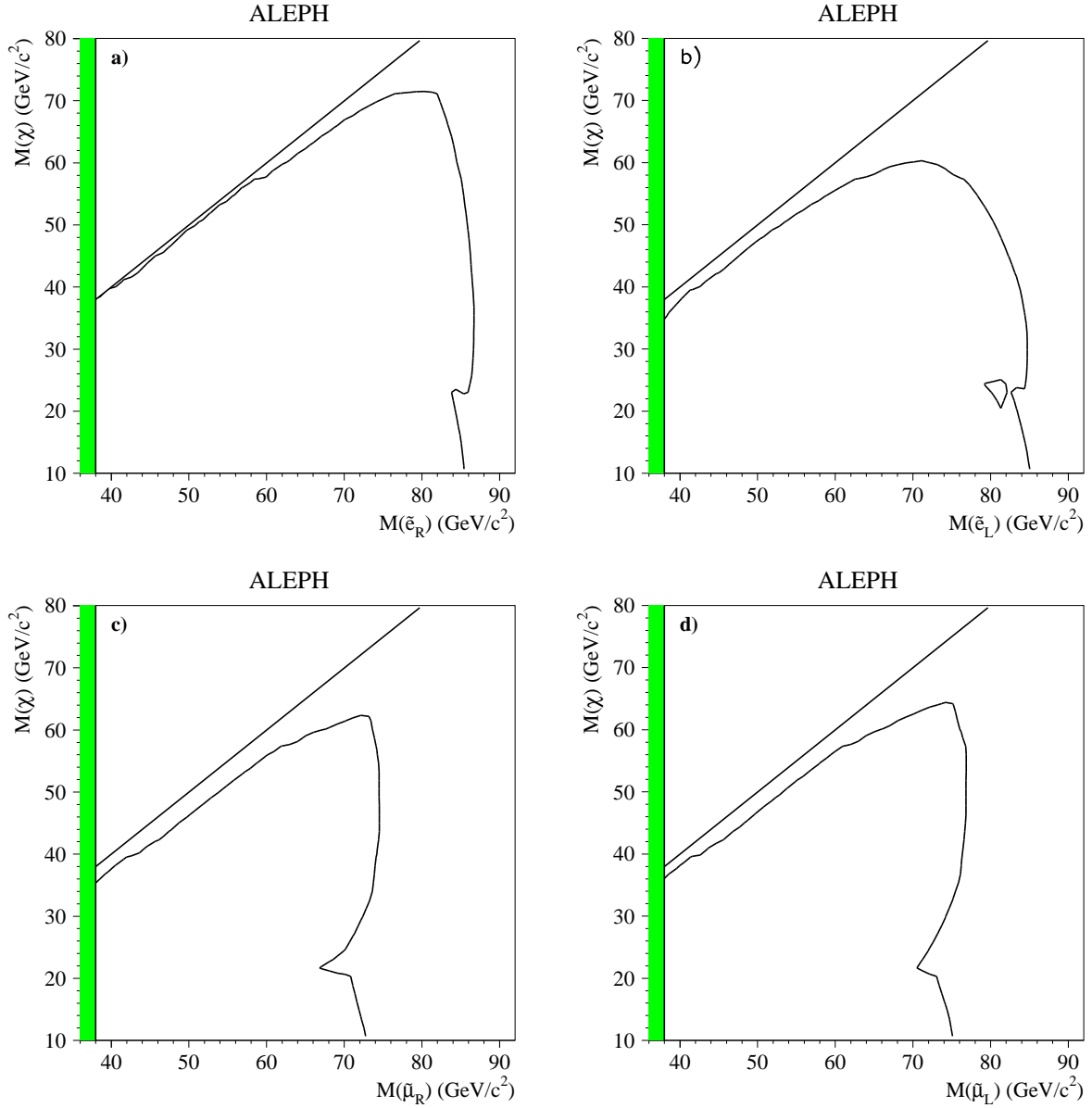


Figure 12: *The 95% C.L. excluded cross-sections for left or right-handed selectrons and smuons decaying indirectly via a dominant $\bar{U}\bar{D}\bar{D}$ operator. The selectron cross-section is evaluated in the region $\mu = -200$ GeV/c² and $\tan\beta = 2$.*

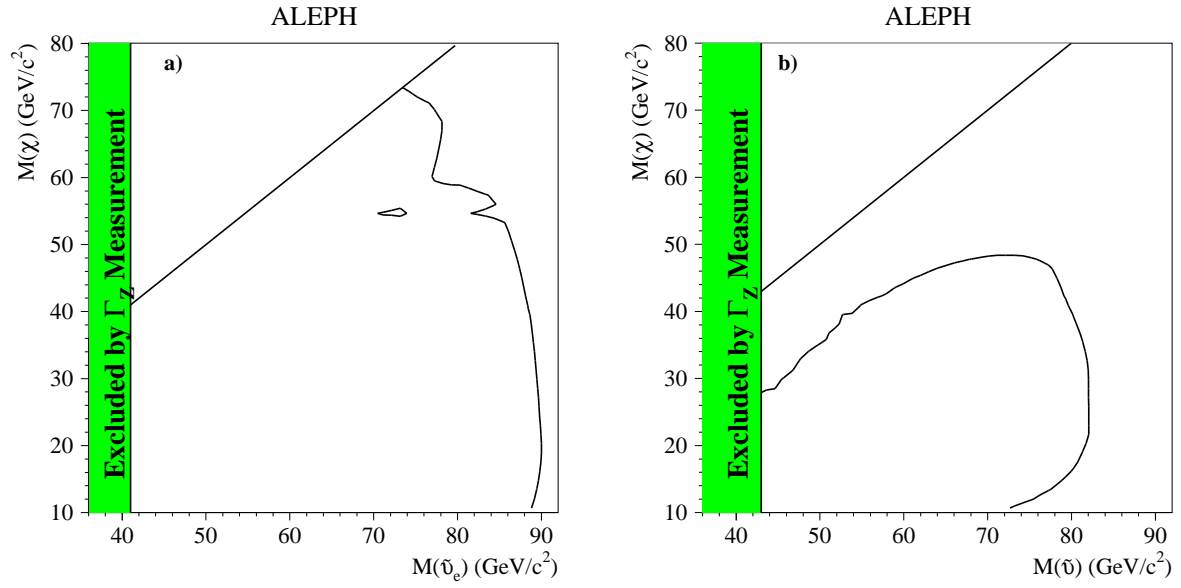


Figure 13: a) The 95% C.L. limit in the $(M_\chi, M_{\tilde{\nu}_e})$ plane for $\tilde{\nu}_e$ decaying indirectly via a dominant $\bar{U}\bar{D}\bar{D}$ operator. The $\tilde{\nu}_e$ cross-section is evaluated in the region $\mu = -200 \text{ GeV}/c^2$ and $\tan\beta = 2$. (The non-excluded island near $M_{\tilde{\nu}_e} = 70 \text{ GeV}/c^2$ is excluded at 90% C.L.). b) The exclusion obtained assuming three mass degenerate sneutrinos.